Received 30 July 2025; revised 17 September 2025; accepted 22 October 2025. Date of publication 30 October 2025; date of current version 10 November 2025.

Digital Object Identifier 10.1109/OJCOMS.2025.3627499

A Joint Power-Aware Spectral Efficient Chunk Allocation, Relay Selection, and Energy Efficient Power Control in OFDMA-PNC Communication

EHSAN ATEFAT DOOST [1,2], FIROOZ B. SAGHEZCHI [3] (Senior Member, IEEE), ALI JAMSHIDI [4,5] (Senior Member, IEEE), ANTONIO NAVARRO [1,2] (Senior Member, IEEE), AND JONATHAN RODRIGUEZ [1,6] (Senior Member, IEEE)

[1] Instituto de Telecomunicações, Campus Universitário de Santiago, 3810-193 Aveiro, Portugal
[2] Departamento de Eletrónica, Telecomunicações e Informática, Universidade de Aveiro, 3810-193 Aveiro, Portugal
[3] Chair for Distributed Signal Processing, RWTH Aachen University, 52074 Aachen, Germany
[4] Department of Communications and Electronics, School of Electrical and Computer Engineering, Shiraz University, Shiraz 71946-84636, Iran
[5] Discipline of Information Technology, Peter Faber Business School, Australian Catholic University, Sydney 2060, Australia
[6] Faculty of Computing, Engineering and Science, University of South Wales, CF37 1DL Pontypridd, U.K.

CORRESPONDING AUTHOR: E. A. DOOST (e-mail: e.atefatdoost@av.it.pt)

This work was supported in part by the Fundação para a Ciência e Tecnologia (FCT), I.P., co-funded by EU funds Instituto de Telecomunicações under Project UIDB/50008/2025; in part by the Fundação para a Ciência e a Tecnologia (FCT-Portugal) under Grant 2021.08263.BD; and in part by the SOVEREIGN Project (funded by the Marie Sklodowska-Curie Actions–MSCA–through the European Union's Horizon Europe Research and Innovation Programme) under Grant 101131481.

ABSTRACT In recent years, besides spectral efficiency (SE), improving energy efficiency (EE) has become a crucial optimization metric in radio resource allocation (RA). This work addresses the joint problem of chunk-level spectral efficient chunk allocation, relay selection, and a subcarrier-level energy-efficient power control algorithm in a multi-user multi-relay orthogonal frequency division multiple access-physical layer network coding (OFDMA-PNC) system. The resulting mixed-integer nonlinear programming (MINLP) problem is NP-hard and computationally intensive. To manage complexity, chunk-level algorithms are used for subcarrier allocation and relay selection. Two MILP solvers and two heuristics handle chunk and relay allocation via Alternating Optimization (AO) method, while power levels are optimized using a convex optimization solver with the Dinkelbach (DKB) algorithm. Simulation results indicate that in a mobile network where user equipment operates at a maximum consumed power of 33.6 dBm, our proposed joint chunk allocation and relay selection method outperforms the heuristic approach, achieving 85% higher SE and a 47% improvement in EE. Additionally, our proposed suboptimal power control algorithm achieves results closely matching the optimal solution obtained using the DKB algorithm, demonstrating its effectiveness in balancing performance and computational efficiency.

INDEX TERMS Chunk allocation, OFDMA-PNC, optimization theory, physical-layer network coding, power control, radio resource allocation, relay selection.

I. INTRODUCTION

To ADDRESS challenges related to coverage, capacity, and energy efficiency, relay communications have been adopted by several standards, such as IEEE 802.11s, IEEE 802.16j, Long-Term Evolution-Advanced (LTE-A), and 5G New Radio (5GNR) [1]. Relay communication networks can be broadly categorized into one-way relay channels (OWRC) and two-way relay channels (TWRC). In this work, we focus on the half-duplex TWRC, where physical-layer network coding (PNC) [2], [3] can significantly improve the spectral efficiency. TWRC with PNC has promising applications in wireless backhauling [4], cell-edge user scenarios [5], smart factory environments, and relay-assisted device-to-device communication in 5G and beyond-5G networks with relays implemented on non-terrestrial platforms such as high-altitude platforms (HAPs) and GEO satellites.

Relays usually operate using amplify-and-forward (AF) or decode-and-forward (DF) protocols. DF-PNC offers higher throughput at low signal-to-noise ratios (SNR) by avoiding noise amplification [6]. PNC frameworks are classified as synchronous or asynchronous [7]. Synchronous PNC ensures symbol and phase alignment using pre-processing techniques, while asynchronous PNC relies on receiver-side post-processing to handle symbol misalignment. This study focuses on the synchronous DF-PNC framework.

To leverage the advantages of PNC systems and efficiently allocate limited wireless resources such as subcarriers, power, and relays, an effective radio resource allocation (RA) scheme is essential for optimizing network performance. RA algorithms typically aim to maximize spectral efficiency (SE) or energy efficiency (EE) while also ensuring fairness among users. The objective is to map users to the available resources in a balanced and efficient manner. Energy efficiency metrics have become vital in reducing the energy consumption of wireless networks [8]. Unlike SE, which emphasizes throughput, EE evaluates the trade-off between energy usage and data delivery efficiency [9], allowing significant energy savings with only minimal throughput compromise [10].

EE metrics are categorized as network-centric (e.g., global EE (GEE)) and user-centric (e.g., weighted minimum user's EE (WMEE), the weighted sum of users' EE (WSEE) [11], weighted product of users' EE (WPEE), and worst-case EE (WCEE) [12]) [13], [14]. GEE, commonly used in downlink scenarios, measures the ratio of total throughput to power consumption, while user-centric metrics focus on optimizing individual EE, typically in uplink transmissions [14].

Orthogonal frequency division multiplexing (OFDM) is a key technology for wireless networks like 4G, 5G, and Wi-Fi. In OFDM-based two-way relay channels, orthogonal frequency division multiple access (OFDMA) enhances performance via subcarrier pairing [15]. Resource allocation in OFDMA relay communications is categorized into per-subcarrier and subcarrier-pairing approaches. While subcarrier pairing offers better performance by exploiting channel dynamics, it is more complex [5]. This work adopts the simpler per-subcarrier policy, assuming channel reciprocity in TDD mode OFDMA.

Relay selection in multi-carrier OFDM systems is typically categorized as subcarrier-wise or chunk-wise. A chunk denotes a group of contiguous subcarriers sharing the same modulation and coding scheme (MCS), ensuring uniform bit error rate (BER) performance across each user's assigned subcarriers. Subcarrier-wise methods optimize each subcarrier individually, yielding fine-grained and outage-optimal performance but at the cost of high system complexity and signalling overhead due to coordination and synchronization among multiple relays [16]. In contrast, chunk-wise methods significantly reduce signalling overhead, enabling simpler implementation [16], [17]. Practical OFDMA systems like LTE and 5G NR adopt chunk-based resource allocation to simplify system design. While most resource allocation strategies in the literature emphasize subcarrier-level granularity, chunk-based relaying, as explored in [16], [18], [19], offers a scalable alternative.

This work explores an OFDMA-PNC-based multi-user, multi-relay system, where the downlink phase is identified as the primary performance bottleneck. Given its suitability for downlink scenarios and reduced computational complexity, the GEE metric is preferred over more complex user-centric alternatives such as WSEE. Accordingly, this work focuses on analyzing the GEE metric.

The study addresses the non-deterministic polynomial-time hard (NP-hard) optimization problem of joint chunk assignment, relay selection, and power control, formulated as a mixed binary integer nonlinear programming (MINLP) problem [20], [21]. To tackle this challenge, a novel mechanism is proposed. The proposed approach integrates power-aware SE-based chunk allocation and relay selection with EE-based power control in an OFDMA-PNC-based multi-user multi-relay system, subject to total power in each chunk and QoS constraints. In particular, the main contributions of this paper can be summarized as follows:

- Unlike previous studies focused on single-relay scenarios and asynchronous PNC frameworks, this work evaluates the GEE performance of multi-user, multi-relay synchronous TWRC with the DF protocol. Our goal is to maximize GEE while ensuring QoS for each user, optimizing relay selection, chunk allocation, and power allocation.
- Existing studies on relay-aided resource allocation for multi-pair two-way relaying typically employ subcarrier-level iterative algorithms for GEE maximization, which are impractical for real-time implementation in multi-carrier OFDM-based PNC systems due to their high computational complexity and signaling overhead [16], [22]. To overcome this limitation, we propose chunk-level algorithms that reduce the search space for subcarrier allocation and relay selection, ensuring alignment with chunk-level relay selection [16]. This formulation enables a joint optimization framework at the chunk level that integrates chunk allocation and relay selection while maintaining subcarrier-level power control for fine-grained performance optimization.
- A pre-determined power scaling factor, computed at the central base station (BS), is introduced for efficient power control during subcarrier suppression in channel inversion-based precoding, enhancing overall energy efficiency.
- The optimization problem in this work is an NP-hard MINLP. We use a branch-and-bound-based algorithm to reduce complexity by dividing variables into discrete, i.e., chunk and relay indices, and continuous, i.e., power levels, categories. Two mixed-integer linear programming solvers and two heuristic algorithms are proposed for chunk and relay allocation using the AO method, followed by a convex optimization solver with the Dinkelbach algorithm for power levels. A suboptimal power control method is also proposed and compared.

The remainder of this paper is organized as follows: Section II reviews the state of the art. Section III introduces the system model, while Section IV formulates the optimization problem. Section V discusses the solution approach for the EE-based optimization problem. Section VI presents the system design, simulation setup, and evaluation results. Finally, Section VII concludes the paper and outlines directions for future research.

II. RELATED WORKS

Energy-efficiency maximization in relay-assisted communication systems has gained significant attention, particularly in the context of joint resource allocation involving subcarrier allocation, relay selection, and power control. This review summarizes the key research contributions in this area, focusing on OWRC and TWRC scenarios.

Generally, the joint optimization problem of subcarrier allocation, relay selection, and power control is NP-hard, requiring a trade-off between accuracy and computational complexity. To address this, two main strategies are used: disjoint-based [23], [24] and joint-based solutions. Disjoint-based solutions (suboptimal) break the problem into three subproblems: relay selection, subcarrier allocation, and power control. This method relaxes subcarrier allocation parameters to indicate the fraction of time each user may occupy a subcarrier [25]. Joint-based solutions (optimal) employ methods such as the Hungarian algorithm [26], branch-and-bound [21], alternating optimization (AO) [27], and weighted one-to-one matching using bipartite graphs [28].

Numerous studies have addressed the optimization of EE in OWRC scenarios by focusing on various joint resource allocation problems, such as subcarrier allocation, relay selection, and power control. For instance, studies such as [26] and [29] integrated subcarrier pairing and allocation with power control. In [26], a two-user single-relay scenario with DF protocol was examined, employing AO method and the Hungarian algorithm for subcarrier pairing. On the other hand, [29] tackled a multi-user single-relay setup with AF protocol, utilizing the Hungarian method for subcarrier pairing and allocation and the Successive Convex Approximation (SCA) and Dinkelbach (DKB) algorithms for power control. These works highlight sophisticated algorithmic approaches to address the complexity of joint resource allocation in OWRC systems. Further, [25] and [30] relaxed binary constraints on subcarrier pairing and allocation indices to real values, applying SCA for convexification and DKB for power control in multi-user single-relay OWRC scenarios with a DF protocol.

In multi-user multi-relay scenarios, the work in [31] tackled the joint problem of relay selection, subcarrier allocation, and power control in a multi-relay OWRC setup with a DF protocol. They utilized heuristic algorithms for relay selection and subcarrier allocation, and the DKB algorithm for power control. Additionally, the work in [27] evaluated the GEE in multi-user OWRC scenarios with multiple relays and DF protocol, addressing the joint problem of relay selection, and power control using various heuristic and optimization techniques.

While OWRC scenarios have been extensively researched, focusing on power control, subcarrier allocation, and relay selection, there is significant interest in optimizing energy efficiency within TWRC systems. TWRC scenarios present unique challenges and opportunities due to bidirectional communication, requiring different optimization strategies. The differences in RA between TWRC and OWRC, particularly in relay selection problems, highlight these distinct optimization needs [32], [33].

The exploration of TWRC scenarios, though less prevalent, has gained attention for its potential to enhance energy efficiency through bidirectional communication. For example, [34] examined the joint problem of subcarrier pairing and power control in an OFDMA-based two-user single-relay TWRC setup with AF protocol, ensuring the desired quality of service (QoS). This work approached the problem in a disjoint manner, using suboptimal algorithms for subcarrier pairing and the DKB algorithm for power control. This disjoint approach reflects a pragmatic strategy to simplify the intricate optimization process.

Expanding the scope to multi-user scenarios, [20] and [35] investigated joint subcarrier pairing, subcarrier allocation, and power control in OFDMA-based multi-user single-relay TWRC systems with AF and DF protocols, respectively. Solving the joint problem in a disjoint manner, these studies employed a combination of suboptimal algorithms for subcarrier operations and the DKB algorithm for power control, further incorporating the SCA method to convexify the problem. Similarly, [36] investigated GEE optimization in an OFDMA-based multi-user, single-relay TWRC scenario using the AF protocol while ensuring the desired QoS. They approached this joint problem in a disjoint manner by first determining fixed optimal subcarrier pairing and allocation through two suboptimal algorithms. To convexify the problem, they used the SCA method, and the DKB algorithm was applied to address the fractional power control problem.

In summary, OWRC research demonstrates a broader exploration of EE maximization across diverse optimization problems and solvers, including AO, SCA, and DKB algorithms. Conversely, TWRC research, while valuable, is less comprehensive and often relies on disjoint methods and suboptimal algorithms, with the integration of relay selection in TWRC scenarios remaining an area for further investigation. Future research could address these gaps by exploring more integrated solutions in TWRC settings. Notably, the problem of joint chunk assignment, relay selection, and power control has not been considered in the context of a multi-user, multi-relay system based on DF-PNC TWRC communication. In this work, we evaluate GEE performance of a multi-user, multi-relay TWRC using the DF protocol. To elaborate on these issues, the system model will be formulated and discussed in the following sections.

III. SYSTEM MODEL AND PRELIMINARIES

A. SYSTEM MODEL

In this work, we consider a multi-pair synchronous OFDMA PNC system, extending the one-pair synchronous OFDM

PNC framework from [7]. The system operates in a single-cell two-way relay (TWR) network, as shown in Fig. 1, comprising M UE pairs (2M UEs total) and R relay nodes (RNs) using a DF-PNC protocol in half-duplex (HD) mode, where relays cannot transmit and receive simultaneously, consistent with [20]. All UEs engage in relay-assisted device-to-device (D2D) communication coordinated by the BS, which centrally collects relevant information for all links to facilitate efficient resource allocation. Uplink and downlink traffic is assumed to be symmetric and must be relayed through one of the R RNs due to the absence of direct links between UEs caused by path loss or shadowing. The channel is considered quasi-static over each scheduling period, with coherence time exceeding the scheduling interval, and channel reciprocity is assumed, valid under time-division duplex (TDD) OFDMA. The system uses OFDMA with N subcarriers, grouped into chunks of N_1 contiguous subcarriers, each assigned to a UE pair through the chunk allocation algorithm described in Section V. For each user pair (A_m, B_m), where $m \in \{1, 2, \ldots, M\}$, we denote by k_{1,A_m} and k_{1,B_m} the subcarriers allocated to A_m and B_m, respectively, during the first hop (uplink phase). Overlapping subcarriers are defined when both users are assigned the same subcarrier, i.e., $k_{1,A_m} = k_{1,B_m} = k_1$. On such subcarriers, both users in the pair transmit simultaneously to the relay, which applies the PNC mapping operation to exploit this intentional interference [37]. The subscript "1" in the notation refers to the first hop (uplink), while the same index "2" is later used to denote the second hop (downlink). To simplify our formulation and optimization problem, we adopt a per-subcarrier policy in which the same subcarrier index is used for both uplink and downlink phases, i.e., $k_1 = k_2$ for each UE pair [15]. As illustrated in Fig. 1, the subcarriers assigned to each pair of links are identified by identical numbering and colors. Furthermore, in both time and frequency domains, the resources allocated to each pair in uplink/downlink are orthogonal to the resources used by other pairs in uplink/downlink links.

Accordingly, like the original PNC signaling [2], in this PNC-based framework, packet exchange is completed in two time slots or phases: the multiple access (MA) phase (uplink) and the broadcast (BC) phase (downlink). Joint resource allocation tasks are carried out during these two consecutive time slots (T_1 and T_2) at the BS.

1) MULTIPLE ACCESS (UPLINK) PHASE

In the first time slot T_1, each of the M paired UEs, denoted as (A_m, B_m), where $m \in \{1, 2, \ldots, M\}$, aims to exchange information with each other through R candidate relay nodes on the same subcarriers ($k_{1A_m} = k_{1B_m} = k_1$). They transmit their signals simultaneously toward the best relay node, which is selected based on an optimization criterion.

To achieve equal amplitude and equal phase (synchronous) arrival of the baseband received signals for each paired UE_{Am} and UE_{Bm}, which is required for PNC mapping operation in QAM modulations [7], we propose a power

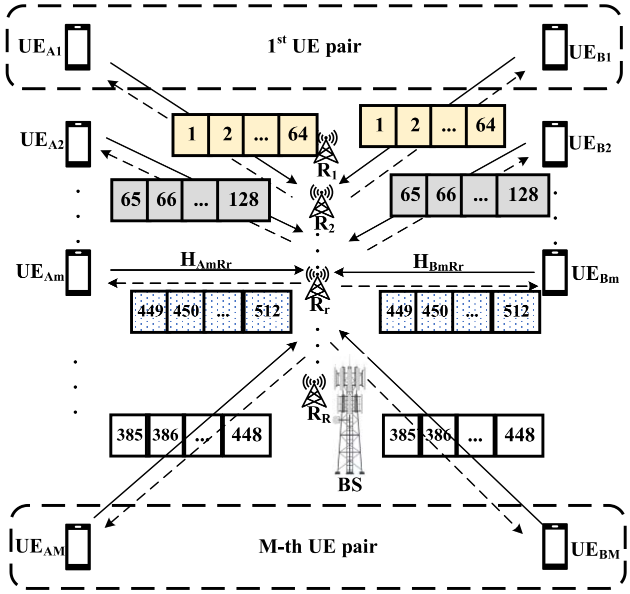

FIGURE 1. System model of the scenario of multi-UE pairs, multi-relay OFDMA-PNC system.

control mechanism. This mechanism customizes the channel inversion-based precoding approach outlined in [38].

Using channel inversion-based precoding, the power and phase adjustments for each paired UE_{A_m} and UE_{B_m} are determined to ensure equal amplitude and synchronous phase at the relay node. The transmission power P_{A_m} and P_{B_m}, as well as the precoding weight factors W_{A_m} and W_{B_m}, are calculated as:

$$\sqrt{P_{A_m}} = \sqrt{\delta_{A_m}}/|H_{A_m R}[k_1]|, \quad \sqrt{P_{B_m}} = \sqrt{\delta_{B_m}}/|H_{B_m R}[k_1]| \tag{1}$$

and

$$W_{A_m} = \exp(-j\angle H_{A_m R}[k_1], \quad W_{B_m} = \exp(-j\angle H_{B_m R}[k_1]. \tag{2}$$

Here, $H_{A_m R}[k_1]$ and $H_{B_m R}[k_1]$ represent the channel coefficients of subcarrier k from UE_{A_m} and $UE_{B_m}$to the relay, respectively. Meanwhile, $|.|$, and $\angle.$ denotes amplitude and phase of (.). Assuming channel reciprocity, we have $H_{A_m R}[k_1] = H_{RA_m}[k_1]$, and $H_{B_m R}[k_1] = H_{RB_m}[k_1]$. In these expressions, δ_{A_m} and δ_{BA_m} are pre-determined power scaling factors, set by the BS. To suppress a minimum number of subcarriers that are in deep fading states, these factors—bounded as $0 < \delta_{A_m} \leq 1$ & $0 < \delta_{B_m} \leq 1$—are applied by the UE pairs for power control during transmission. This approach avoids unnecessary power amplification over highly attenuated subcarriers and improves the system's energy efficiency. Using these parameters, the transmitted signals in Phase 1 for each paired UEs of UE_{Am} and UE_{Bm} are expressed as:

$$\sqrt{P_{A_m}} W_{A_m} X_{A_m}[k_1] = \frac{\sqrt{\delta_{A_m}}\ X_{A_m}[k_1]}{H_{A_m}[k_1]} \tag{3}$$

and

$$\sqrt{P_{B_m}} W_{B_m} X_{B_m}[k_1] = \frac{\sqrt{\delta_{B_m}}\ X_{B_m}[k_1]}{H_{B_m}[k_1]}. \tag{4}$$

Here, $X_{A_m}[k_1]$ and $X_{Bm}[k_1]$ are the transmitted symbols from nodes A_m and B_m, respectively on the subcarrier k_1, where $k_1 = 1, 2, \ldots, N$, and $m = 1, 2, \ldots, M$. These symbols use the same order of equally likely M-QAM modulation constellations, with an average symbol power of

$$P_{s1}[k_1] = E\Big(|X_{A_m}[k_1]|^2\Big) = E\Big(|X_{B_m}[k_1]|^2\Big) = 2\frac{M-1}{3}d^2, \tag{5}$$

where $2d = 2\sqrt{3E_b(\log_2 L)/(M-1)}$ denotes the Euclidian distance between the neighboring constellations in inphase and quadrature components of the M-QAM signal which are L-PAM signals ($L = \sqrt{M}$), given an energy of E_b per bit [39]. Since using channel inversion-based precoding may largely increase power consumption and thus deteriorate its EE performance [40], it is necessary to devise a way to improve its EE performance by considering all of these factors. Using the maximum transmit power (P_{max}) constraint on each chunk, the UEs use a truncated channel inversion power control mechanism such as the subcarrier suppression method as in Section V-A ([38]).

To ensure that the signals received at the relay from each paired UE are aligned in both amplitude and phase, the following condition must be satisfied:

$$\sqrt{P_{A_m}} W_{A_m} H_{A_m R}[k_1] = \sqrt{P_{B_m}} W_{B_m} H_{B_m R}[k_1]. \tag{6}$$

After substituting P_{A_m}, P_{B_m}, W_{A_m}, and W_{B_m} parameters from (1), and (2), in (6) we have

$$\delta_{A_m} = \delta_{B_m} = \delta_m[k_1],\ 0 < \delta_m[k_1] \leq 1 \tag{7}$$

in which $\delta_m[k_1]$ is defined as in (44) in the Appendix.

Using this channel inversion-based power control mechanism, at the r-th selected relay (hereafter referred to simply as the r-th relay, though we continue to use R_r interchangeably where appropriate to improve readability), as discussed in [7], the resulting superimposed received signal on the subcarrier k becomes:

$$Y_{R,r}[k_1] = \sum_{m=1}^{M} \sqrt{\delta_m[k_1]}\ (X_{A_m}[k_1] + X_{B_m}[k_1]) + N_{R,r}[k_1],$$
$$\forall k \epsilon \{1, 2, \ldots, N\} \tag{8}$$

where $N_{R,r}[k_1]$ is the receiver noise at the relay node r which is additive white Gaussian noise (AWGN) and has a complex normal distribution as $N_{R,r} \sim N_C(0, N\sigma_t{}^2)$, where N is the Fast Fourier Transform (FFT) size, $\sigma_t{}^2 = N_0/2$ is the noise variance per subcarrier, and N_0 is the power spectral density of the noise. We assume that channel coefficients are invariant during each of the two time slots of PNC signaling. The channel coefficients, which comprise two components of the large-scale and small-scale fading components are modelled as in [7]. It should be noted that in OFDMA signaling, each UE pair m is allocated only one chunk of the N subcarriers (consisting of N_1 subcarriers), where the subcarriers within that chunk carry nonzero values, while the remaining subcarriers are set to zero and reserved for other UE pairs to transmit their data.

In our OFDMA-PNC framework extended from the OFDM-based framework created based on Wi-Fi standard as in [7], each chunk has $N_1 = N/M$ subcarriers ($N_1 = 64$) subcarriers. Since noise is added in the time domain, it affects all subcarriers. To estimate the SNR per subcarrier and the average SNR in OFDMA symbols, since each UE pair (A_m, B_m) operate on the same frequency bands (chunks), while other UE pairs (A_n, B_n) with $n \neq m$, use orthogonal subcarriers, with a noise equivalent bandwidth of $W_1 = W/M$, the frequency domain SNR at the relay corresponding to the m-th UE pair contribution on each subcarrier k_1 is given by:

$$SNR_{R,r}[k_1] = \frac{E(|\sqrt{\delta_m[k_1]}(X_{A_m}[k_1] + X_{B_m}[k_1])|^2)}{N.\sigma_t{}^2/M}$$
$$= \frac{M.P'_s \delta_m[k_1]}{\sigma_t{}^2} \tag{9}$$

in which P'_s is the average symbol power of the superposed signal at the relay before PNC mapping operation, calculated as follows. For example, in our synchronous OFDM-PNC system, if each of the transmitted signals has a 16-QAM constellation, the resulting superimposed signal has a 49-QAM constellation since using [41, Table 2], each of the I and Q components of the superimposed signal has 7-PAM constellations. The minimum distance, defined as the Euclidean distance between adjacent constellation points in the 49-QAM constellation, is $d_{min} = 2d$. Hence, the average symbol power is as in [39],

$$P'_s = 35d^2. \tag{10}$$

Furthermore, since the transmit power of both source and relay nodes has an upper limit and cannot have an arbitrarily high value, we consider the parameter P_{max} as the maximum available total transmit power for each chunk assigned to each UE pair. We assume that $P_{Amax} = P_{Bmax} = P_{max}$, and this maximum power is equal for all UE pairs. To respect the maximum, transmit power limit of the UEs, we must suppress some subcarriers that are in deep fading states not to be scheduled in our RA process. To relate the maximum level for the transmit power (P_{max}) into the maximum level for the consumed power (P'_{max}) we use $P'_{max} = P_{max}/\eta_m$, where η_m is the m-th UE pair power amplifier (PA) efficiency parameter.

2) BROADCAST (BC) PHASE

In the second time slot (phase), the selected relay node (through relay selection algorithm) performs PNC mapping on each subcarrier as in [7], converting $Y_{R,r}[k_1]$ in (8) to $X_{R,r}[k_2]$ and then broadcasts $X_{R,r}[k_2]$ toward both paired-nodes (A_m, B_m) on the same subcarriers. To define the links between each pair of UEs and different relays, two sets of integer binary variables including the subcarrier allocation indicator, $\tau_m(k_1, k_2)$, and the relay selection indicator, $\rho_{r,m}(k_1, k_2)$, are introduced as follows. The variable $\tau_m(k_1, k_2)$ takes the value of 1 if the subcarrier pair (k_1, k_2) is allocated to the m-th UE pair, and 0 otherwise. Furthermore, the binary variable $\rho_{r,m}(k_1, k_2)$ assumes the value of 1 when the relay R_r is selected for communication with the m-th UE pair, and 0 otherwise.

Using the per-subcarrier policy, as mentioned before, utilizing the same subcarriers ($k_2 = k_1$) for both uplink and downlink phases for each UE pair [15], the received signals at A_m and B_m on subcarrier k_1 are given by:

$$Y_{A_m}[k_1] = \sum_{m=1}^{M} \sqrt{P_R}\rho_{r,m}(k_1, k_1)\tau_m(k_1, k_1) .H_{A_m}[k_1]X_R[k_1] + N_{A_m}[k_1], \tag{11}$$

and

$$Y_{B_m}[k_1] = \sum_{m=1}^{M} \sqrt{P_R}\rho_{r,m}(k_1, k_1)\tau_m(k_1, k_1).H_{B_m}[k_1]X_R[k_1] +N_{B_m}[k_1]. \tag{12}$$

For simplicity, we denote $\rho_{r,m}(k_1, k_1)$ as $\rho_{r,m}(k_1)$ and $\tau_m(k_1, k_1)$ as $\tau_m(k_1)$ in the subsequent formulations. Furthermore, without loss of generality, we assume $k_1 = k$. To provide a compact representation, we define a three-dimensional binary allocation index $x_{m,k,r} = \rho_{r,m}(k)\tau_m(k)$. When $x_{m,k,r} = 1$, it means that relay r is used to relay the signals of the m-th UE pair utilizing the subcarrier k. Otherwise, we have $x_{m,k,r} = 0$.

Assuming channel state information (CSI) is known at the receiving end, each node can omit its own transmitted signal component from the received signal and recover its desired (its pair's user's) data.

In the following subsection, we formulate GEE optimization problem.

IV. FORMULIZATION OF THE OPTIMIZATION PROBLEM

The GEE is defined as [11],

$$GEE = \frac{R_{sum}(\overline{\mathbf{P}})}{P_T(\overline{\mathbf{P}})} \tag{13}$$

for which $R_{sum}(\overline{\mathbf{P}})$ and $P_T(\overline{\mathbf{P}})$ are the total system rate and the total power consumption, which are defined as in Sections IV-A and IV-B, respectively. The vector $\overline{\mathbf{P}} = [P_1, P_2, \ldots, P_k, \ \ldots, P_N]$ represents the system power on N subcarriers for which $P_k = [P_{A_m}[k], P_{B_m}[k], P_{R,r}[k]]$ is the vector of the system power on the subcarrier k.

A. ACHIEVABLE SUM-RATE ESTIMATION IN THE MULTIPAIR TWRC

Using the Shannon capacity formula, the achievable sum-rate of the TWRC using DF-PNC relaying protocol on each subcarrier k, for one round of communications with two time slots is given by [42],

$$R_{sum,m} = R_{A_mB_m} + R_{B_mA_m} = \min\{C_{A_mR}, C_{RB_m}\} +\min\{C_{B_mR}, C_{RA_m}\} \tag{14}$$

where $R_{A_mB_m}$ and $R_{B_mA_m}$ denote the achievable rate from node A_m to node B_m and from node B_m to node A_m, respectively, each of which is expressed in the unit of [bits/sec/Hz]. In (14), C_{X_mR} and C_{RX_m} are the link capacities between the source/destination node X_m and the relay node, R_r, (where $X_m \in \{A_m, B_m\}$) in the first and the second time slots respectively as follows.

$$C_{X_mR} = \frac{1}{2}\log_2\left(1+SINR_{R,X_m}\right), X_m, X_n \in \{A_m, B_m\}; m \neq n$$
$$C_{RX_m} = \frac{1}{2}\log_2\left(1+\frac{|H_{RX_m}|^2 P_{s1}[k]P_R[k]}{\sigma^2_{X_m}}\right), \quad X_m, X_n \in \{A_m, B_m\}; m \neq n \tag{15}$$

where C_{X_mR} is the achievable rate (capacity) for X_m. The factor 1/2 is due to two time slots of TWRC [37], while each node only transmits in one time slot of two. Since using DF-PNC protocol [20], the transmission of each pair of (A_m, B_m) are on the same overlapping subcarriers, the B_m contribution is as an interference in the link $A_m \rightarrow R_r$. From (3)–(5), the signal-to-interference plus noise ratio (SINR) at the relay R_r due to each of the UEs in the m-th paired UEs (A_m, B_m) sharing the same chunk subcarriers is as

$$SINR_{R,X_m} = \frac{P_{s1}[k]|H_{X_mR}|^2 P_{X_m}}{|H_{X_nR}|^2 P_{X_n} + \sigma^2_R} = \frac{P_{s1}[k]\delta_m[k]}{\sigma^2_R} \tag{16}$$

where σ^2_R is the relay side receive noise power. Since each UE pair (A_m, B_m) are working on the same chunks while other pairs (A_n, B_n) with $n \neq m$ are working on orthogonal subcarriers to this pair, the interference term contribution of $\left|H_{X_nR}\right|^2.P_{X_n}$ in SINR is omitted in (16). Indeed, using precoding-based OFDM-PNC, the AWGN channel condition is achieved as in (8), and capacity of (15), would be as:

$$C_{X_mR} = \tfrac{1}{2}\log_2\left(1+\tfrac{P_{s1}[k]\delta_m[k]}{\sigma^2_R}\right),$$
$$C_{RX_m} = \frac{1}{2}\log_2\left(1 + \frac{|H_{RX_m}|^2 P_{s1}[k]P_R[k]}{\sigma^2_{X_m}}\right). \tag{17}$$

Assuming $\sigma^2_{X_m} = \sigma^2$ for all the UEs, by plugging (17) into (14), and since the logarithm function is a monotonically increasing function, we obtain

$$R_{sum,m} = \log_2\left(1 + \min\left\{\frac{P_{s1}[k]\delta_m[k]}{\sigma^2_R}, \frac{|H_{RB_m}[k]|^2 P_{s1}[k]P_R[k]}{\sigma^2_{X_m}}, \frac{|H_{RA_m}[k]|^2 P_{s1}[k]P_R[k]}{\sigma^2_{X_m}}\right\}\right). \tag{18}$$

Due to the existence of min(.) in (18), as we will see in the next subsections, the GEE problem in (13) belongs to the class of max-min programming problem [14]. Through some simplifications, we can convert this problem to a max programming problem as follows to speed up the optimization algorithm's convergence rate. For the simplifications, we make some assumptions as in the following.

Assuming equity of the noise variances in all the receivers, $\sigma^2_{X_m} = \sigma^2_R = \sigma^2$, as discussed in [43], in optimal power allocation scheme, relay broadcast rates/capacities ($C^{PNC}_{RB_m}$) should always be greater than the uplink rates/capacities (C_{X_mR}), which from (18), this corresponds to the inequality of

$$P_{s1}[k]\delta_m[k] \le P_{s1}[k]P_R[k]\left|H_{RB_m}[k]\right|^2,$$
$$P_{s1}[k]\delta_m[k] \le P_{s1}[k]P_R[k]|H_{RA_m}[k]|^2, \forall k\epsilon\{1, 2, \dots, N\}. \tag{19}$$

Otherwise, the UE_{A_m}, and UE_{B_m} must put more power in the uplink phase. Indeed, this is useless when the relay cannot broadcast at those rates in the downlink phase. Hence, using (19), the equation (18) can be simplified as below:

$$R_{sum,m} = \log_2\left(1+\frac{P_{s1}[k]\delta_m[k]}{\sigma^2_R}\right) \tag{20}$$

Subject to: C_1: $\delta_m[k] \le P_R[k] \min\{\left|H_{RB_m}[k]\right|^2, \left|H_{RA_m}[k]\right|^2\}$, $\forall k\epsilon\{1, 2, \dots, N\}$.

Now, from C_1 in (20), we can write $P_R[k]$ variable as

$$P_R[k] \ge \frac{\delta_m[k]}{\min\{\ |H_{RB_m}[k]|^2\ \ |H_{RA_m}[k]|^2\}}, \tag{21}$$

where $P_R[k]$ is the transmitted power at the relay.

Using (20), the total sum-rate in the multipair TWRC is as

$$R_{sum,Total}(\overline{P}) = \sum_{r=1}^{R}\sum_{m=1}^{M}\sum_{k=1}^{N_{used}} x_{m,k,r}\ R_{sum,m}(k). \tag{22}$$

B. TOTAL POWER CONSUMPTION IN THE MULTIPAIR TWRC

The total power consumption in multi-pair multi-relay TWRC can be expressed as [11]

$$P_T(\overline{P}) = \sum_{m=1}^{2M}\left(P_{c,m} + \sum_{k=1}^{N} P_{s1}[k]\frac{P_m[k]}{\eta_m}\right) + \sum_{r=1}^{R}\left(P_{c,r} + \sum_{k=1}^{N}\frac{P_{R,r}[k]}{\eta_r}\right), \tag{23}$$

in which $P_m[k]$ ($= P_{A_m}[k]$, or $= P_{B_m}[k]$), and $P_{c,m}$ are respectively transmit power and circuit power of the m-th UE pair, while $P_{R,r}[k]$ and $P_{c,r}$ are the transmit power and circuit power on the subcarrier k of the r-th relay, respectively [13]. The consumed power of the relays ($\frac{P_{R,r}[k]}{\eta_r}$) and the source nodes (UEs) ($\frac{P_m[k]}{\eta_m}$) are limited by $P'_{R,rMax}$, and P'_{A_mMax} respectively. We assume that $P_{A,max} = P_{B,max} = P_{max}$, $P'_{max} = P'_{max}/\eta_m$, and this maximum power is equal for all UE pairs. The parameters η_m and η_r are the m-th UE pair and R_r-th (simply denoting as r-th) relay power amplifier (PA) efficiency respectively.

Using the channel inversion-based precoding as in (1), equation (23) can be rewritten as

$$P_T(\overline{P}) = \sum_{m=1}^{2M}\left(P_{c,m} + \sum\nolimits_{k=1}^{N}\frac{\delta_m P_{s1}[k]}{|H_{X_mR}[k]|^2}\frac{1}{\eta_m}\right) + \sum_{r=1}^{R}\left(P_{c,r} + \sum_{k=1}^{N}\frac{P_{R,r}[k]}{\eta_r}\right). \tag{24}$$

To avoid excessive power consumption on subcarriers experiencing deep fading (i.e., $\left|H_{X_mR}[k]\right| <$ Threshold), we apply the subcarrier suppression method described in Section V-A, whereby such subcarriers are deactivated and excluded from transmission. Here, the Threshold represents a minimum acceptable channel gain level, below which reliable transmission cannot be guaranteed without requiring excessive transmit power.

C. GEE OPTIMIZATION PROBLEM

To define GEE under the QoS constraints of the sum rate, we start our formulizations at the subcarrier-level. From (13), (22), and (24), the GEE problem can be formulated as

P_1: refer to the bottom of the next page.

$$\begin{aligned}
&\text{s.t.}C_1: \sum_{r=1}^{R}\sum_{m=1}^{M} x_{m,k,r} = 1\ x_{m,k,r}\in\{0,1\}, \forall k\epsilon\{1, 2, \dots, N_{used}\};\\
&C_2: \sum_{m=1}^{M}\sum_{k=1}^{N} x_{m,k,r} \le N_{Rmax}\ \ \forall r\epsilon\{1, 2, \dots, R\};\\
&C_3: \sum_{k=(m-1)\times 64+1}^{m\times 64}\frac{P_{R,r}[k]}{\eta_r} \le P'_{RrMax}\ \ \forall r\epsilon\{1, 2, \dots, R\}, \forall m\epsilon\{1, 2, \dots, M\};\\
&C_4: \sum_{k=(m-1)\times 64+1}^{m\times 64}\frac{P_{A_m}[k]}{\eta_m} = \sum_{k=(m-1)\times 64+1}^{m\times 64}\frac{\delta_m[k]}{|H_{A_mR}[k]|^2}\frac{1}{\eta_m} \le P'_{max};\\
&\sum_{k=(m-1)\times 64+1}^{m\times 64}\frac{P_{B_m}[k]}{\eta_m} = \sum_{k=(m-1)\times 64+1}^{m\times 64}\frac{\delta_m[k]}{|H_{B_mR}[k]|^2}\frac{1}{\eta_m} \le P'_{max},\\
&\forall m\epsilon\{1, 2, \dots, M\};\\
&C_5: P_R[k] > \frac{\delta_m[k]}{\eta_r \times \min\{\left|H_{RB_m}[k]\right|^2\ \left|H_{RA_m}[k]\right|^2\}}, \forall k\\
&C_6: P_{R,r}[k] \ge 0, \forall\ r,\ k
\end{aligned} \tag{25}$$

where $N_{used,m} \le N$ is the number of used (active) subcarriers in the channels of the m-th UE pairs which is determined in the subcarrier suppression process as in Section V-A. Furthermore, as discussed before, when the binary variable $x_{m,k,r} = 1$, it means that relay r is used to relay the signals of the m th UE pair utilizing subcarrier k. Otherwise, we have $x_{m,k,r} = 0$. To avoid interference, this binary variable must satisfy the above-mentioned constraint of C_1 and C_2. The constraint C_1 mandates that each subcarrier k, can be allocated to only one UE pair. The constraint C_2 ensures that each relay r, can be selected up until N_{Rmax} times for different UE pairs (A_m, B_m). The constraints C_3 to C_6 represent individual power constraints at each node. It should be noted that since $N_{used,\ m}$ subcarriers are activated in OFDM signaling, the $\frac{1}{N_{used,\ m}}$ factor appears in the numerator of (25), (i.e., $R_{sum-OFDMA}(\overline{P})$). In (25), as said before, the parameter P_{max} is the maximum available total power for each chunk assigned to each UE pair.

On the other hand, the optimization variable in the numerator of (25) is $x_{m,k,r}$, while the numerator is independent of the variable $P_{R,r}[k]$. Conversely, the denominator's only optimization variable is $P_{R,r}[k]$. Consequently, SE optimization is performed for subcarrier and relay selection tasks, focusing on the numerator. Meanwhile, EE-based optimization is applied to the power control task, considering GEE metric as defined in (25) at the subcarrier level. To implement chunk-level relay selection and chunk allocation within our OFDMA-PNC system framework, which is the focus of this work, the resource allocation problem in (25) is reformulated accordingly, while power control remains at the subcarrier level.

D. CHUNK-LEVEL RESOURCE ALLOCATION FORMULATION

In the proposed chunk-level processing, we employ a fixed power scaling factor δ_m for each chunk (see (43) in the Appendix) and enforce equal modulation order and equal transmit power ($P_{s1}[k] = P_{s1}$) across all subcarriers within a chunk to ensure equal-amplitude and equal-SNR arrivals at the relay, as described in (8) and (9). Under these uniform modulation and equal power constraints, the achievable rate is lower than the Shannon capacity. In particular, the $\log_2(.)$ term in the Shannon expression assumes adaptive modulation across subcarriers, fully exploiting per-subcarrier channel variations, which is not applicable in our framework. Hence, it cannot be used as the actual data rate.

Furthermore, because we employ a subcarrier suppression method (see Section V-A), only the active subcarriers in each chunk contribute to data transmission. Let $R_{sum}(m, c, r)$ denote the number of active subcarriers for the link between the m-th UE pair and relay r on chunk c. Following [8], we define an SE-like metric based on $R_{sum}(m, c, r)$, which represents the effective transmission rate (bit/s). This metric provides finer granularity for optimization in the $R_{sum}(m, c, r)$ search space by using integer-valued active subcarriers, rather than relying on the real-valued $\log_2(.)$ term $\left(\log_2\left(1+\frac{P_{s1}\delta_m}{\sigma_R^2}\right)\right)$ and naturally incorporates chunk-level constraints and subcarrier suppression.

By applying this SE-like metric to the GEE formulation, we obtain a simplified optimization problem that captures the effective transmission rate relative to the total consumed power. This leads to the following reformulation:

P_2: refer to the bottom of this page.

$$\text{s.t. } C'_1: \sum_{r=1}^{R}\sum_{m=1}^{M} x_{m,c,r} = 1\ x_{m,c,r}\in\{0,1\}, \forall c\epsilon\{1,2,\ldots,C\};$$

$$C'_2: \sum_{m=1}^{M}\sum_{k=1}^{N} x_{m,c,r} \leq N_{Rmax}\ \ \forall r\epsilon\{1,2,\ldots,R\};$$

$$C'_3 \text{ to } C'_6: \text{like } C_3 \text{ to } C_6, \text{with replacing } \delta_m[k] \text{ with } \delta_m \tag{26}$$

Here, $S(m, c, r) = bR_{sum}(m, c, r)/T_s$ represents the sum rate for the link between the m-th pair and relay r on chunk c, where T_s is the OFDM symbol duration, and $b = \log_2(Q)$ is the number of bits per QAM symbol with order Q. $R_{sum}(m, c, r)$ denotes the total number of active subcarriers of the m-th UE pair, which is determined from the number of good subcarriers—a function of δ_m—as described in Section V-A. The constraint C'_1 ensures that each chunk c can be allocated to only one UE pair, while constraint C'_2 limits each relay r to being selected at most N_{Rmax} times across different UE pairs (A_m, B_m). Like (25), the remaining constraints represent the individual power constraints at each node, where C'_3, C'_4 and C'_5 also incorporate subcarrier suppression method as described in Section V-A.

If different UEs require different data rates, a fair resource allocation strategy is to distribute radio resources proportionally to their rate constraints. Let $\overline{R}_m$ denote the required data rate for data transmission between A_m and B_m. Following [44], we introduce the following constraint to (26):

$$C'_7: \sum_{k=1}^{N} \min\{R_{A_m-B_{m,\ k}}, R_{B_m-A_{m,\ k}}\} = S(m,c,r) \geq \overline{R}_m = \overline{R}_0;\ \ m\epsilon\{1,2,\ldots,\ M\} \tag{27}$$

where $\overline{R}_0$ (in bits/sec) represents the QoS threshold. Since $R_{sum}(m, c, r)$ denotes the total number of active subcarriers for the m-th UE pair—determined via the subcarrier suppression method described in Section V-A—an alternative constraint can be used:

$$C'_7: R_{sum}(m,c,r) \geq \overline{S}_1 \tag{28}$$

where $\overline{S}_1$ (in subcarriers/chunk) represents the QoS threshold for the minimum number of active subcarriers allocated to the m-th UE pair's chunk.

Due to the existence of binary variable $x_{m,c,r}$, and real-valued $P_{R,r}[k]$ variable, the optimization problem of joint chunk allocation, multi-relay selection, and power control of P_2 in (26) is a MINLP problem, that is NP-hard and computationally prohibitive, making it challenging to find the global optimum solution [20], [21].

V. SOLVING THE EE-BASED OPTIMIZATION PROBLEM

The joint optimization problem of (26) is NP-hard, so finding the optimal solution is not computationally feasible and trade-offs must be made regarding computational complexity and performance. To address the joint optimization problem with three optimization variables, i.e., chunks, relay indices, and power levels, by assuming a constant value for the δ_m parameter as described in equation (52), and the constraint inequality of (19), we decouple the δ_m parameter from the chunk and the relay indices and the $P_{R,r}[k]$ variable. This approach enables us to separate the optimization variables into distinct groups, reducing the complexity of the joint optimization problem.

Instead of searching through all possible combinations of chunk-level chunk allocation, relay selection, and subcarrier-level power control, which may involve unnecessary dimensions of the search space, we utilize a branch-and-bound based algorithm. We divide the optimization variables into discrete and continuous variables, thereby decoupling the joint optimization problem into two distinct groups:

1. Joint chunk and relay indices: A discrete optimization problem, which can be solved using mixed-integer linear programming.

2. Relay power variable: A continuous optimization problem.

To jointly address the above-mentioned problems, we adopt an alternating optimization (AO) approach as described in [27] and illustrated in Fig. 2. In this framework, the chunk and relay indices are optimized first, followed by power allocation at the subcarrier level using a convex optimization solver (e.g., the Dinkelbach algorithm). The AO algorithm operates iteratively, optimizing one parameter at a time while keeping the others fixed, and proceeds for up to n_{AO} iterations. Since the power allocation step does not affect relay or subcarrier selection, it is executed outside the AO loop. This layered structure ensures that the overall optimization can be efficiently completed within the channel coherence time, leveraging predicted CSI. It should be noted that in Fig. 2, R_{sum} represents the computed good chunk matrix. Furthermore, C^*_m and R^*_m denote the optimally (or suboptimally) selected chunk and relay, respectively, for the m-th UE pair, and $\overline{P^*_R}$ represents the optimal power allocation vector for the corresponding selected relays at the allocated chunks.

UEs transmit power is determined by channel inversion-based power control, while relays power is optimized for energy efficiency. To improve reliable channel-inversion OFDM-PNC, subcarrier suppression is integrated with relay selection and chunk allocation, following the strategy in [46]. The proposed algorithm includes three main stages as in the following subsections.

Remark (Tensor, Matrix and Vector Notation): Throughout this paper, bold uppercase letters denote tensors or matrices (e.g., X, while plain symbols with indices denote their elements (e.g., $X(m, c, r)$). For example, $R_{sum} \in R^{M\times C\times R}$ represents the tensor of active subcarriers across UE pairs, chunks, and relays, while $R_{sum}(m, c, r)$ denotes the element corresponding to the m-th UE pair, chunk c, and relay r.

Matrices are treated as two-dimensional tensors. For example, $Y \in R^{M\times C}$ is a matrix with elements $Y(m, c)$. Vectors are considered as one-dimensional matrices; for example, $\overline{Z} \in R^{1\times M}$ denotes a row vector with elements $Z(1, m)$.

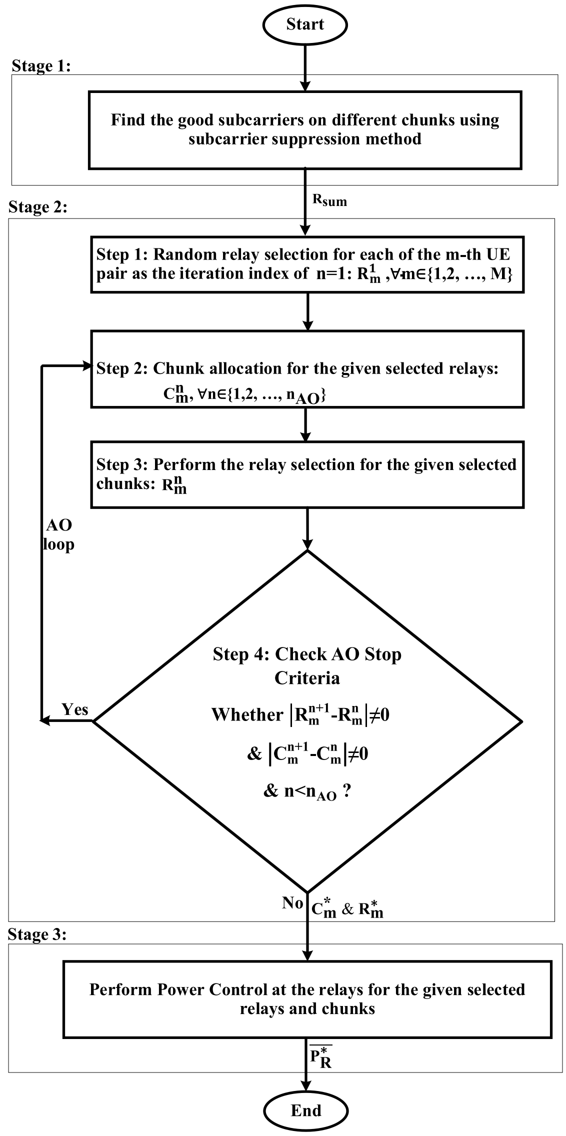

FIGURE 2. Flow chart showing the optimization of the joint problem of chunk allocation, and relay selection using AO algorithm, followed by a power control algorithm.

A. STAGE 1) INITIALIZE THE PROCESS BY FINDING GOOD SUBCARRIERS ON DIFFERENT CHUNKS

This preprocessing stage computes $R_{sum}(m, c, r)$, the three-dimensional tensor of good chunks, determined by their total number of good subcarriers, by applying the joint subcarrier suppression method [45] through the following four steps.

1) First, each relay $R_r \in \{1, 2, \ldots, R\}$ operates in parallel to calculate the channel frequency response matrix for each paired UEs (A_m, B_m) of Fig. 1, on different $A_m \rightarrow R_r$ and $B_m \rightarrow R_r$ links (for each $m = 1, 2, \ldots, M$), as follows, and the data are saved in two matrices $H_{A_m R_r}$, and $H_{B_m R_r}$ at the central BS node, and all the matrices corresponding to different relays are saved in two tensors $H_{A_m R}$ and $H_{B_m R}$. For instance, in the case of 16 UEs (8 paired UEs:

8×64 subcarriers), we have

$$\mathbf{H_{A_mR_r}} = \begin{bmatrix} H_{1,1} & H_{1,2} & \cdots & H_{1,512} \\ H_{2,1} & H_{2,2} & \cdots & H_{2,512} \\ \cdot & \cdot & \cdots & \cdot \\ \cdot & \cdot & \cdots & \cdot \\ \cdot & \cdot & \cdot & \cdot \\ H_{M,1} & H_{M,2} & \cdots & H_{M,512} \end{bmatrix},$$

$$\mathbf{H_{B_mR_r}} = \begin{bmatrix} H'_{1,1} & H'_{1,2} & & H'_{1,512} \\ H'_{2,1} & H'_{2,2} & \cdots & H'_{2,512} \\ \cdot & \cdot & \cdots & \cdot \\ \vdots & \vdots & \cdots & \vdots \\ H'_{M,1} & H'_{M,2} & & H'_{M,512} \end{bmatrix} \tag{29}$$

for which there is M rows corresponding to the $M = 8$ UEs, and $N = 512$ columns corresponding to N subcarriers of the OFDMA system. Moreover, we assume that the channels are reciprocal, i.e., $H_{A_mR} = H_{RA_m} = H_{A_m}$, and $H_{B_mR} = H_{RB_m} = H_{B_m}$, as in the TDD mode of OFDMA access technology, and quasi-static (i.e., the path gains are regarded as a constant within scheduling periods). $|H_{m,k}|^2$ and $|H'_{m,k}|^2$ are channel gains corresponding to the m-th paired UEs (A_m, B_m) at the subcarrier k.

2) Next, employing the variable δ_m as defined in (52), each relay R_r, operating in parallel, calculates power levels corresponding to the subcarriers of links $A_m \rightarrow R_r$ and $B_m \rightarrow R_r$ and saves it in two matrices $P_{A_mR_r}$, and $P_{B_mR_r}$ as

$$\mathbf{P_{A_mR_r}} = \delta_m P_{s1} \begin{bmatrix} 1/|H_{1,1}|^2 & 1/|H_{1,2}|^2 & \cdots & 1/|H_{1,512}|^2 \\ 1/|H_{2,1}|^2 & 1/|H_{2,2}|^2 & \cdots & 1/|H_{2,512}|^2 \\ \vdots & \vdots & \cdots & \vdots \\ \vdots & \vdots & \cdots & \vdots \\ 1/|H_{M,1}|^2 & 1/|H_{M,2}|^2 & 1/|H_{M,512}|^2 & \end{bmatrix},$$

$$\mathbf{P_{B_mR_r}} = \delta_m \mathbf{P_{s1}} \begin{bmatrix} 1/|\mathbf{H}'_{1,1}|^2 & 1/|\mathbf{H}'_{1,2}|^2 & 1/|\mathbf{H}'_{1,512}|^2 & \\ 1/|\mathbf{H}'_{2,1}|^2 & 1/|\mathbf{H}'_{2,2}|^2 & \cdots & 1/|\mathbf{H}'_{2,512}|^2 \\ \cdot & \cdot & \cdots & \cdot \\ \vdots & \vdots & \cdots & \vdots \\ 1/|\mathbf{H}'_{M,1}|^2 & 1/|\mathbf{H}'_{M,2}|^2 & 1/|\mathbf{H}'_{M,512}|^2 & \end{bmatrix}. \tag{30}$$

After computing the per-link power allocation matrices $P_{A_mR_r}$ and $P_{B_mR_r}$, each relay forwards its respective matrix to the BS. At the BS, these are organized into two three-dimensional tensors, $P_A \in R^{M\times C\times R}$ and $P_B \in R^{M\times C\times R}$. The element $P_A(m, k, r)$ corresponds to the power metric of user A_m in the m-th UE pair on subcarrier k via relay r, while $P_B(m, k, r)$ represents the power metric of its paired user B_m on the same subcarrier and relay.

3) Now, we perform subcarrier suppression method using Algorithm 1 in the BS to find the set of jointly active subcarriers for each UE pair and relay. The procedure begins with initialization, where the power metrics of all subcarriers are computed using (30), and the active and joint subcarrier tensors are initialized. In the active subcarrier selection phase, subcarriers within each chunk are sorted in ascending order by their power metrics and iteratively added to the active set until the maximum transmit power constraint (P_{max}) is satisfied. If including a subcarrier would exceed this power budget, it is suppressed by assigning

Algorithm 1: The Joint Subcarrier Suppression Algorithm

Input:
- Maximum power constraint P_{max}.
- Power metrics $P_A \in R^{M\times C\times R}$, and $P_B \in R^{M\times C\times R}$ as in (30).
- Number of relays R.
- Number of chunks C.
- Number of subcarriers per chunk N_1.

Output:
- $T_{JAS} \in R^{M\times C\times R}$: Tensor of joint active subcarriers.
- $R_{sum} \in R^{M\times C\times R}$: Tensor of total number of joint active subcarriers per chunk.

Step 1: Initialization
1. Compute power metrics $P_A(m, k, r)$, and $P_B(m, k, r)$ using (30).
2. Initialize active subcarrier sets
- $A_{AS}(m, k, r) = 0$, $B_{AS}(m, k, r) = 0$ (Tensor of active subcarriers for UE group A_m, and B_m, respectively).
- $T_{JAS}(m, k, r) = 0$ (joint active subcarriers)
- $R_{sum}(m, c, r) = 0$ (joint active subcarriers per chunk)

Step 2: Finding Active Subcarriers for Individual Chunks
For each relay $r = 1, \ldots, R$:
  For each UE pair $m = 1, \ldots, M$:
    For each chunk $c = 1, \ldots, C$:
      Sort subcarriers $k \epsilon c$ by ascending power metrics
      Set total allocated power of A_m, and B_m to zero
      For each subcarrier $k \epsilon c$:
        If (total allocated power of A_m on subcarrier $k + P_A(m, k, r)) \leq P_{max}$:
          Select k into the active set $A_{AS}(m, k, r) = 1$
          Update total allocated power of A_m
        Else:
          Supresst k ($A_{AS}(m, k, r) = 0$)
        End If
        If (total allocated power of B_m on subcarrier $k + P_B(m, k, r)) \leq P_{max}$:
          Select k into the active set $B_{AS}(m, k, r) = 1$
          Update total allocated power of B_m
        Else:
          Supresst k ($B_{AS}(m, k, r) = 0$)
        End If
      End For
    End For
  End For
End For

Step 3: Construction of Joint Active Subcarriers for Individual Chunks
For each relay $r = 1, \ldots, R$:
  For each UE pair $m = 1, \ldots, M$:
    For each chunk $c = 1, \ldots, C$:
      For each subcarrier $k \epsilon c$:
        If ($A_{AS}(m, k, r) = 1$) AND ($B_{AS}(m, k, r) = 1$), (i.e., k is active for both UEs)
          Set $T_{JAS}(m, k, r) = 1$
        End If
      End For
      Update $R_{sum}(m, c, r)$ =count of joint active subcarriers in chunk c
    End For
  End For
End For

a zero entry in the active subcarrier tensor. The power corresponding to suppressed subcarriers is not redistributed; instead, these subcarriers are excluded from the scheduling process. This approach ensures strict compliance with the power constraint while retaining only the most efficient subcarriers. Finally, in the construction phase, the algorithm identifies the overlap between the active subcarriers of the two UEs in each pair, thereby forming the joint active subcarrier tensor, and updates a per-chunk count of the total number of jointly active subcarriers. Through this structured process, the algorithm ensures strict compliance with the transmit power constraint while preserving the most effective subcarriers for data transmission, thereby achieving power-constrained and performance-oriented subcarrier selection under practical fading conditions.

4) Next, to include the QoS constraints C'_7 from (28) into our optimization process, we construct the tensor of good chunks, $R_{sum}^{QoS}(m, c, r)$, based on the calculated $R_{sum}(m, c, r)$. A "good chunk" is defined as a chunk in which the total number of active subcarriers exceeds the QoS-limited minimum rate (active subcarriers) for each chunk in the tensor $R_{sum}(m, c, r)$, corresponding to each relay r:

$$R_{sum}^{QoS}(m, c, r) = \begin{cases} R_{sum}(m, c, r) & \text{if } R_{sum}(m, c, r) \geq \overline{S}_1 \\ 0 & \text{Otherwise.} \end{cases} \quad (31)$$

By this, we eliminate low-quality chunks to guarantee QoS for all the UE pairs. Furthermore, we assume that the total number of active UE pairs (M) is equal to the number of available chunks (C).

B. STAGE 2) AO ALGORITHM FOR JOINT CHUNK AND RELAY ASSIGNMENT

This stage handles the discrete optimization of resource allocation by iteratively alternating between chunk assignment and relay selection—the fundamental steps of joint resource mapping prior to power control optimization, as depicted in AO Algorithm 2. This process is subdivided as follows.

1) PERFORM THE RANDOM RELAY SELECTION

Perform random- or distance-based relay selection for each UE pair, allowing each relay to be selected up to N_{Rmax} times. Then, proceed to the chunk allocation step as in the following.

2) SE-BASED CHUNK ALLOCATION FOR THE GIVEN SELECTED RELAYS

Once relays are assigned to UE pairs in the previous step (Section V-B.1), we perform chunk-level allocation to maximize SE on each relay, using power-optimized chunks based on the subcarrier-suppression mechanism from Stage 1 (Section V-A).

First, using the calculated chunks tensor $R_{sum}(m, c, r)$ from Stage 1 (Section V-A), we create chunk matrix $R_{sum}(m, c)$ for the selected relays determined in Section V-B.1, as

$$R_{sum}(m, c) = \begin{bmatrix} R'_{1,1}, R'_{1,2}, & \cdots & R'_{1,C} \\ R'_{2,1}, R'_{2,2}, & & R'_{2,C} \\ \vdots & \ddots & \vdots \\ R'_{M,1}, R'_{M,2}, & \cdots & R'_{M,C} \end{bmatrix} \quad (32)$$

where rows are UE pairs and columns are chunks (with the corresponding relays).

Then, we can select the c-th chunk for the m-th UE pair using the following chunk allocation optimization problem to guarantee the maximum SE with the following constraints.

$$c_m^* = \text{Arg max} \sum_{i=1}^{M} \sum_{j=1}^{C} R_{ij} x_{ij}$$

Subject to

$$C_1: \sum_{j=1}^{C} x_{ij} = 1, \forall\, i \in \{1,\ 2,\ \ldots,\ M\}$$

$$C_2: \sum_{i=1}^{M} x_{ij} = 1, \forall\, j \in \{1,\ 2,\ \ldots,\ C\} \quad (33)$$

in which $\{R_{ij}\} \in R_{sum}(m, c)$ as given in (32). $X = \{x_{ij}\}$ is the chunk allocation variable matrix which has binary elements as $x_{ij} \in \{0, 1\}$, where $x_{ij} = 1$ means that UE pair i is paired with the chunk j, and $x_{ij} = 0$ means otherwise.

Algorithm 2: AO Algorithm

Initialize iteration index $n = 1$
Initialize SelectedRelays(1), SelectedChunks(1)
repeat
  $n = n + 1$
  Compute SelectedChunks(n) for the given relays (refer to subsection V-B.2)
  Compute SelectedRelays(n)for the given chunks (refer to subsection V-B.3)
  DeltaRelays =abs(SelectedRelays(n)− SelectedRelays(n − 1))
  DeltaChunks = abs(SelectedChunks(n)−) SelectedChunks(n − 1)
  Save iteration index and SE(n)
  If SE(n) > SE(n − 1) **then**
    Update suboptimal solution with SE(n)
  End If
until (DeltaRelays = = 0 AND DeltaChunks = = 0)
OR (n reaches maximum, n_{AO})
If converged **then**
  Proceed to Stage 3: Power Control (refer to subsection V-C)
Else
  Repeat step of subsection V-B.2 & step of subsection V-B.3
End If

a) ACCURATE SOLUTION: To solve the chunk allocation optimization problem (33) which is a mixed-integer linear programming (MILP) optimization problem with respect to x_{ij} variable, we can use a standard convex optimization solver (software) such as MATLAB, CVX [47], CPLEX [48], etc. In this work, we use MATLAB intlinprog command [49]. Traditionally, the branch-and-bound (BB) method is used to solve MILP problems, but its complexity grows exponentially with the number of variables, making it unsuitable for large problems, [50], [51]. To tackle this issue, in the following, we propose a heuristic algorithm.

b) A HEURISTIC SOLUTION: In this algorithm, instead of using MATLAB intlinprog command for our MILP problem, we propose a greedy-like heuristic algorithm with three steps as follows.

Step 1) Based on (32), we create a good chunk matrix for the given relays as $R_{sum}(m, c)$, we save a copy of the $R_{sum}(m, c)$ as a $R_{sum2}(m, c)$ for the middle computations in step 3 in the following.

Step 2) Then, we perform summation on elements of each row as

$$R''_{i,1} = \sum_{j=1}^{C} R'_{i,j}, \forall i \in \{1, 2, \ldots, M\} \tag{34}$$

Using these results, we construct the column vector R'' by stacking all elements of $R''_{i,1}$:

$$R'' = \begin{bmatrix} R''_{1,1} \\ R''_{2,1} \\ \cdot \\ \cdot \\ \cdot \\ R''_{M,1} \end{bmatrix}. \tag{35}$$

Step 3) Next, we sort the rows (UEs) of R'' based on their good chunks from min to max: starting with $m' = 1$-st UE pair which has the minimum number of good chunks and assign the best chunk from the $R_{sum2}(m, c)$ matrix corresponding this UE row to this pair. Then, we continue the chunk assignment operation for the remaining UE pairs. Since each chunk can be selected once only, after assignment of each chunk, the selected chunk from the $R_{sum2}(m, c)$ matrix must be deleted by putting -1 value in all the elements of the column corresponding to the selected chunk. Through repeating step 3, the chunks (with the corresponding assigned relay) will be allocated to the UEs.

Assume that we have selected the best chunk for each m-th UE pair of (A_m, B_m) as in the above subsection and denote it as C_m. Next, we will consider the problem of relay selection.

3) SE-BASED RELAY SELECTION FOR THE GIVEN SELECTED CHUNKS

With the aim of maximizing SE on the given chunks, we propose a chunk-level multiple-relay selection as follows while the available chunks were power optimal using the subcarrier-suppression mechanism as in Stage 1.

First, using the calculated "good chunks" tensor $R_{sum}(m, c, r)$ from Stage 1 (Section V-A), we construct the "good chunks" matrix $R_{sum}(m, r)$ for the selected chunks corresponding to different m-th UE pairs, as determined in Section V-B.2. The matrix $R_{sum}(m, r)$ is represented as:

$$R_{sum}(m, r) = \begin{bmatrix} R''_{1,1}, R''_{1,2}, & \ldots & R''_{1,R} \\ R''_{2,1}, R''_{2,2}, & & R''_{2,R} \\ \vdots & \ddots & \vdots \\ R''_{M,1}, R''_{M,2}, & \cdots & R''_{M,R} \end{bmatrix}, \tag{36}$$

where rows are UE pairs and columns are relays (with corresponding assigned chunks). Meanwhile, the users index corresponding different chunks $(C_1, C_2, \ldots, C_C)$ must be saved in another dimension of the new tensor, to be used in the final step.

Then, we can select the r-th relay for the m-th UE pair by solving the following relay selection optimization problem, which ensures the maximum SE while satisfying the given constraints:

$$\begin{aligned} & r^*_m = \operatorname{Arg\,max} \sum_{i=1}^{M} \sum_{j=1}^{R} R_{ij} x_{ij}; \\ & \text{Subject to} \\ & C_1: \sum_{i=1}^{M} x_{ij} \le N_{Rmax}; \ \forall\, j \in \{1, 2, \ldots, R\} \\ & C_2: \sum_{j=1}^{R} x_{ij} = 1; \forall\, i \in \{1, 2, \ldots, M\} \end{aligned} \tag{37}$$

where $\{R_{ij}\} \in R_{sum}(m, r)$ as given in (36), and $X = \{x_{ij}\}$ is the relay assignment matrix with binary elements, where $x_{ij} \in \{0, 1\}$. Constraint C_1 ensures that each relay can be selected no more than N_{Rmax} times, while constraint C_2 guarantees that each chunk can be assigned to only one UE pair.

a) ACCURATE SOLUTION: To solve the relay selection optimization problem (37) which is a MILP optimization problem with respect to x_{ij} variable, like in chunk allocation process, we use MATLAB optimization toolbox and intlinprog command [49]. As said before; to tackle the exponential complexity of MILP solvers such as the branch-and-bound algorithm, we propose a sub-optimal heuristic algorithm as follows.

b) A HEURISTIC SOLUTION: In this algorithm, we propose a greedy like heuristic algorithm with three steps as follows.

Step 1) Based on (36), we determine good chunk matrix $R_{sum}(m, r)$ for the selected chunks corresponding different m-th UEs, we save a copy of the $R_{sum}(m, r)$ as a $R_{sum2}(m, r)$ for the middle computations in step 3.

Step 2) Then, since each chunk can be selected once only, while each relay can be selected up until N_{Rmax} times, we perform summation on elements of each column of $R''_{i,j}$. This operation creates a new matrix $R'''_{i,1}$, computed as:

$$R'''_{i,1} = \sum_{j=1}^{R} R''_{i,j}, \forall i \in \{1, 2, \ldots, M\} \tag{38}$$

Using this result, we construct the column vector R''' by stacking all elements of $R'''_{i,1}$:

$$R''' = \begin{bmatrix} R'''_{1,1} \\ R'''_{2,1} \\ \cdot \\ \cdot \\ \cdot \\ R'''_{M,1} \end{bmatrix} \tag{39}$$

Step 3) Next, we sort the R''' (chunks) vector elements based on their good chunks (subcarriers) from min to max: starting with $m' = 1$-st chunk which has the minimum number of good chunks and assigns the best relay corresponding to this chunk column from the $R_{sum2}(m, r)$ matrix to this pair. Then, we continue the relay selection operation for the remaining chunks (with the corresponding UE pairs). Furthermore, since each relay can be selected N_{Rmax} times, so for higher than this for each selected relay, we delete it from the $R_{sum2}(m, r)$ by putting -1 instead of R_{ij} values row of the overreach selected relay.

Through repeating Step 3, the relays (with the corresponding preassigned chunk) will be assigned to the UEs.

4) CHECK AO STOP CRITERIA

Then, we check the AO stop criteria as in Algorithm 2, to check whether the relay selection and chunk allocation results are converged, remain constant or reach a maximum iteration.

Meanwhile we save the iteration index and the corresponding SE value. For the next iteration, if the resulted SE is higher than the previous one, we keep this iteration and the corresponding SE as the suboptimal solution.

If it is converged, we go to Stage 3 (Section V-C) i.e., power control algorithm; otherwise, we repeat Stage 2 (Section V-B) iteratively using AO algorithm (Algorithm 2) to arrive with the convergence criteria. Then, we construct the selected transmit power matrices for the UE pairs (i.e., P_{A_m}, P_{B_m} as in (30)) and then go to Stage 3 (Section V-C) as in the next subsection.

C. STAGE 3) EE-BASED POWER ALLOCATION

After performing relay selection and chunk allocation at the chunk level, as described in the previous subsections, the links are defined. The integer variables in (26) are omitted, leaving power control as the remaining optimization problem. This task is performed at the subcarrier level to leverage the multicarrier diversity potential of OFDM signaling. The resulting problem is formulated as a fractional programming (FP) problem. To address this FP optimization problem, we propose two methods: (1) the DKB algorithm and (2) a suboptimal approach, as outlined below.

1) OPTIMAL SOLUTION USING DINKELBACH ALGORITHM

Since in our subcarrier suppression method, we considered the constraint of C'_4 in (26); hence, our only optimization variable in (26) is $P_{R,r}[k]$. Representing $\overline{P_R} = [P_{R,r}[1], P_{R,r}[2], \ldots, P_{R,r}[k], \ldots, P_{R,r}[N]]$ as the vector of the selected relays' power on N subcarriers, the objective in (26) thus takes the form $\frac{\text{Num}}{\text{Den}(\overline{P_R})}$, where the numerator, Num, is a constant with respect to the relay power variable $\overline{P_R}$, and the denominator, $\text{Den}(\overline{P_R})$, is a function solely of the $\overline{P_R}$. According to [27], [52], a constant numerator is affine, and since the denominator is convex with respect to the optimization variable (due to its linear summation form of $P_{R,r}[k]$ variable [52]), the overall objective function is semi-concave. Furthermore, the associated constraints are convex, ensuring that the optimization problem P_2 in (26) can be effectively solved using fractional programming techniques such as the Dinkelbach algorithm [53] or the Charnes–Cooper transformation [54].

In this work, the Dinkelbach algorithm [53] is employed for GEE maximization. The flowchart for Algorithm 3 illustrates the interaction between the DKB algorithm and its embedded sub-algorithms, notably the iterative exchange between the q-function estimator and the nonlinear optimization solver until convergence is achieved.

The DKB algorithm operates via the alternating optimization (AO) technique [55] as shown below:

- The inner problem updates the variable $F(q_n) = \text{Num}\left(\overline{P_R}(n)\right) - q_n \text{Den}(\overline{P_R}(n))$ in each iteration $n \epsilon \{1, 2, \ldots, n_{AO}\})$ by solving for a fixed, iteratively updated parameter q_n.
- The outer problem subsequently updates $q_{n+1} = \frac{\text{Num}\left(\overline{P_R^*}(n)\right)}{\text{Den}(\overline{P_R^*}(n))}$ using the solution from the inner step q_n.

Here, $\overline{P_R^*}(n) = \overline{P_R}(n)$ is the optimally calculated relay powers vector at iteration n, and $\text{Num}\left(\overline{P_R^*}(n)\right) = \text{Num}$, is a constant with respect to the relay power variable vector $\overline{P_R}$. This parametric reformulation converts the initial fractional programming (FP) problem into a sequence of convex optimization problems indexed by q_n [56], enabling reliable and efficient computation of the unique global optima using solvers such as MATLAB's optimization toolbox, CVX [47], or the Lagrange dual method as in [11], [55].

For constrained linear multivariable optimization in MATLAB, fmincon function [49] is used as the primary solver, specifically designed for nonlinear problems with constraints. The DKB algorithm achieves super-linear convergence by halting iterations once the change $\Delta q_n = |q_n - q_{n-1}|$ is less than the chosen tolerance ε, as defined in [31]. It should be noted that $\overline{P_R^*}$ is the optimal power allocation after DKB algorithm convergence.

2) SUBOPTIMAL SOLUTION

Since after performing the relay selection and chunk allocation, our only optimization variable in (26) is $P_{R,r}[k]$,

Algorithm 3: Dinkelbach Algorithm for GEE as in P_2

Input: Maximum tolerance $\varepsilon = 0.001$, maximum iterations $n_{DKB} = 20$
Output: Optimal power allocation $\overline{P_R^*}$ for GEE maximization
Initialize iteration index $n = 0$
Initialize $q_n = 0$, $\Delta q_n = 1$
While $\Delta q_n \geq \varepsilon$ & $n < n_{DKB}$:
  Solve the convex optimization subproblem $F(q_n) = \mathrm{Num}(\overline{P_R}(n)) - q_n \mathrm{Den}(\overline{P_R}(n))$ using a standard convex optimization tool
  Compute $F(q_n) = \mathrm{Num}\left(\overline{P_R^*}(n)\right) - q_n \mathrm{Den}(\overline{P_R^*}(n))$
  Update $q_{n+1} = \frac{\mathrm{Num}\left(\overline{P_R^*}(n)\right)}{\mathrm{Den}(\overline{P_R^*}(n))}$
  $n = n + 1$
  $\Delta q_n = |q_n - q_{n-1}|$
End while
$\overline{P_R^*} = \overline{P_R^*}(n)$, the optimal power allocated to the relays that were selected for different UE pairs

moreover, the numerator in (26) has a constant value, while the denominator only variable is $P_{R,r}[k]$. Therefore, to maximize the GEE we need to minimize the denominator. Furthermore, since $P_{R,r}[k]$ has positive values, the denominator is an increasing function. Hence, the minimum point of the denominator can be obtained by finding the minimum values for $P_{R,r}[k]$ and substituting these values into the GEE equation of (26). Using (21), we can find optimal $P_{R,r}[k]$ as:

$$P_{R,r}{}^*[k] = P_{R,rMin}[k] = \frac{\delta_m}{\min\{\ |H_{RB_m}[k]|^2,\ |H_{RA_m}[k]|^2\}} \quad \forall k \epsilon \{1, 2, \ldots, N_{used}\}. \tag{40}$$

Hence, no need to use a solver to solve this optimization problem, if we set $P_{R,r}{}^*[k] = P_{R,rMin}[k]$ using (40), on different subcarriers, GEE in (26) will be equal to its maximum value. Furthermore, to guarantee the constraint C'_3 in (26), we sort the $P_{R,r}{}^*[k]$ values on each chunk in the increasing order, and only select the subcarriers that total power on that chunk reaches to the $P'_{RrMax} = P_{RrMax}/\eta_r$ value. This needs further subcarrier suppression in the power control process also. However, using the DKB algorithm does not need further subcarrier suppression. Hence, if the relay node has enough processing capacity, DKB method is preferable.

Thus, there is no need to use a solver to solve this optimization problem if we set $P_{R,r}{}^*[k] = P_{R,rMin}[k]$ using (40) for different subcarriers. In this case, the GEE in (26) will reach its maximum value. Furthermore, to satisfy the constraint C'_3 in (26), we sort the $P_{R,r}{}^*[k]$ values within each chunk in ascending order and select only the subcarriers until the total power in that chunk reaches $P'_{RrMax} = P_{RrMax}/\eta_r$. This requires additional subcarrier suppression during the power control process. However, when using the DKB algorithm, no further subcarrier suppression is needed. Therefore, if the relay node has sufficient processing capacity, the DKB method is the preferable choice.

It should be noted that Stages 1–3 must be updated within the channel coherence time, ensuring that good subcarrier identification, AO-based allocation, and DKB-based power optimization are executed adaptively to maintain reliable performance under time-varying channel conditions.

VI. SYSTEM DESIGN AND NUMERICAL EXPERIMENTS

A. SYSTEM DESIGN PARAMETERS

To evaluate the resource allocation algorithms within our multiuser multi-relay OFDMA-PNC framework, illustrated in Fig. 1, we consider a single-cell system comprising $2M = 16$ user equipment (UEs), organized into $M = 8$ UE pairs, and $R = 8$ relays, all deployed within a 1 km × 1 km square area. The UEs are randomly distributed across the area, while the relays (RNs) are fixed and positioned at coordinates given by $500e^{j(\pi/4)r}$, for $r = 1, 2, \ldots, R$, relative to a reference coordinate system centered at the BS, which is located at the center of the square.

Each UE is associated with a selected relay node, and each relay can be selected by at most $N_{Rmax} = 1$ UE pair. The system adopts the Wi-Fi 6 IEEE 802.11ax standard frame format, employing OFDMA with $N = 512$ subcarriers [57]. These subcarriers are grouped into chunks of N_1 contiguous subcarriers (e.g., $N_1 = 64$), with each chunk allocated to a UE pair using a chunk allocation algorithm, as described in the previous subsections. Accordingly, the system can support $M = N/N_1 = 8$ UE pairs.

The UEs and relays are equipped with $N_T = 1$ antenna each. All propagation channels are generated as a baseband realization of the Rayleigh faded tapped-delay-line (TDL-C) model, a realistic 5G channel model in the Urban Micro (UMi) Street-canyon scenario presented in [58]. Furthermore, assuming that receiver-side amplification fully compensates for large-scale fading, we ignore path loss effects in our simulations.

All paired UEs are configured with the same maximum feasible power consumption per chunk, denoted as $P_{max} \in [0.1 - 10]$ W. Each UE also has a hardware-dissipated power of $P_{c,Max} = 0.1$ W (as in [27]), and the UEs power amplifier efficiency of $\eta_m = 0.3$. Relay nodes are designed with a maximum feasible power consumption per chunk of $P_{R,Max} \geq P_{max}$, which exceeds that of UEs, and has a hardware-dissipated power of $P_{c,r,Max} = 0.1$ W. The power amplifier efficiency for the relays is $\eta_r = 0.35$. The maximum number of iterations for the DKB algorithm, n_{DKB} is set to 20, while the AO algorithm, n_{AO} is configured with 200 iterations. All simulations were conducted over 1000 independent channel realizations to ensure statistical reliability.

We consider OFDMA design parameters as summarized in Table 1.

To set the δ_m parameter for link design, we utilize [7], where $\delta_m = 1$ was assumed. By fixing the transmit power and adjusting the noise power $(\sigma_{t1}{}^2)$ to achieve the desired

TABLE 1. Design parameters.

Parameters	Value	
Bandwidth (W_2)	20 MHz for OFDMA	
Distance between Subcarriers (Δf)	78.125 KHz	
$T_{fft}=4\times T_{CP}=T_{symbol}-T_{CP}$	512 (B/Δf)	66.67 µs
Cyclic prefix ($T_{CP}=1/(4\times\Delta f)$)	128 samples	3. 2 µs
Symbol Length: $T_{symbol}=T_{fft}+T_{CP}=5\times T_{CP}$	512+128=640	12.8 µs
Number of subchannels (chunks) (UE pairs)	8	
Number of data subcarriers/Subchannel	48	
Number of pilot subcarriers/Subchannel	4	
Total Number of subcarriers/Subchannel	64	
Modulation	16-QAM	

SNR, δ_{Min} can be calculated as follows. Receiver noise is modeled as AWGN with per-subcarrier power $\sigma_{t1}{}^2 = B_n.N_0.NF$, wherein B_n is the subcarrier bandwidth, N_0 is the noise power spectral density, and NF is the noise figure. Using $\delta_m = 1$ in [7] and assuming $\delta_{Min1} = 1$, we calculate $\sigma_{t1}{}^2$ and determine $N_{01} = \sigma_{t1}{}^2/B_{n1}.NF_1$.

For comparison between the OFDM-PNC in [7] and the OFDMA-PNC in this work, we derive $\delta_{Min1}/\delta_{Min2}$ using (51) (in Appendix):

$$\frac{\delta_{Min1}}{\delta_{Min2}} = \frac{8P'_{s2}(N_{01}W_1NF_1SNR)_{Min1}}{P'_{s1}(N_{02}W_2NF_2SNR)_{Min2}} \tag{41}$$

Assuming uniform 16-QAM modulation across all subcarriers and setting $P_{s1} = 1$ in equation (5), equation (41) can be simplified accordingly. For 16-QAM, based on equation (10), the average symbol power is $P'_s = 3.5$, with a minimum symbol distance $d = \sqrt{0.1}$. According to [7], for 16-QAM with 64 subcarriers (OFDM, $W_1 = 10$MHz), achieving a bit error rate (BER) of 10 requires a minimum SNR of $SNR_{R,Min} = 15$dB. Using 16-QAM for OFDMA ($SNR_{Min1} = SNR_{Min2} = 10^{1.5}$) and assuming identical receiver noise ($N_{01} = N_{02}$, and $NF_1 = NF_2$), (41) reduces to:

$$\frac{\delta_{Min1}}{\delta_{Min2}} = \frac{8W_1}{W_2} \tag{42}$$

Thus, from (42), with $W_1 = 10$MHz and $W_2 = 20$MHz (Table 1), we find $\delta_{Min2} = 0.25$. This value of $\delta_{Min} = \delta_{Min2}$ is used throughout our simulations.

B. IMPACT OF THE RELAYS AND THE UE'S TRANSMIT POWER ON THE SE AND EE

Fig. 3, and Fig. 4 show the SE, and EE of the multiuser OFDMA-PNC system respectively versus the maximum transmit power of each UEs (P_{max}) in the TDL-C channel for different regimes of δ_m value, as in (52).

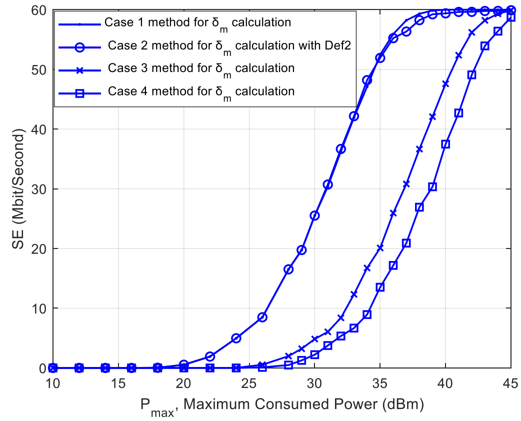

FIGURE 3. (Average) SE results versus P_{max} with different regimes of δ_m.

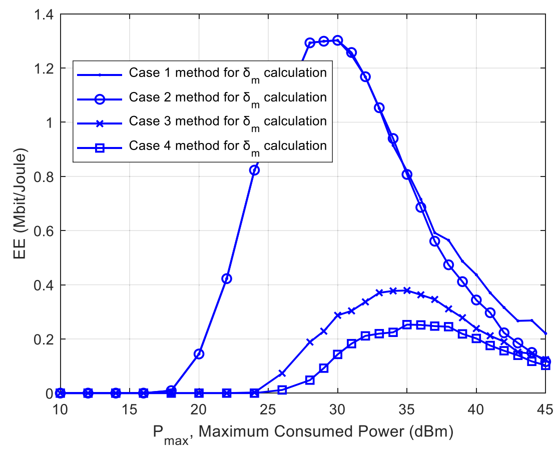

FIGURE 4. (Average) EE results versus P_{max} with different regimes of δ_m.

To identify the optimal operating point for selecting δ_m values, we employ the following experimental approach, using (52). First, we define two boundary regions, representing the lower and upper bounds, and a central region, representing the middle values for the δ_m parameter. These regions are sorted from the minimum to the maximum value, as shown in the following case illustrations.

Case 1: Near the lower point for δ_m using uplink SNR (δ_{Min}): To satisfy $\delta_{Min} \leq \delta_m$, we choose $\delta_m = \delta_{Min}$ (from (51));

Case 2: Middle point for δ_m using (43) and (52);

Case 3: Near the upper point for δ_m : To satisfy $\delta_m \leq \delta'_{m,Max}$, we choose $\delta_m = \delta'_{mMax}$;

Case 4: Higher than the upper point for δ_m ($\delta_m > \delta'_{m,Max}$): $\delta_m = 1.5\delta'_{mMax}$.

In Figs. 3 and 4, we observe the variation of the resulting SE and EE, respectively, using different values of δ_m as in cases 1-4, while changing the P_{max} parameter. The dotted, circle, cross, and square lines represent the aforementioned values. Here, to respect (21), we assume $P_{R,Max} = P_{max}$, to employ all the activated subcarriers/chunks through AO-based joint chunk and relay selection algorithms. As can be seen from these two figures, there is a trade-off between EE

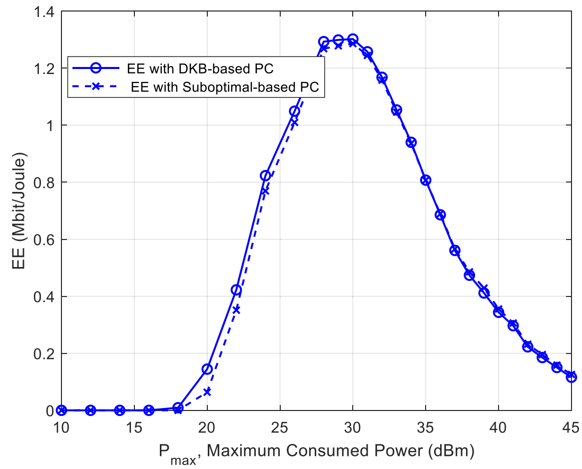

FIGURE 5. (Average) EE results versus P_{max}: using suboptimal method vs. DKB algorithm power control solvers with δ_m as in case 2.

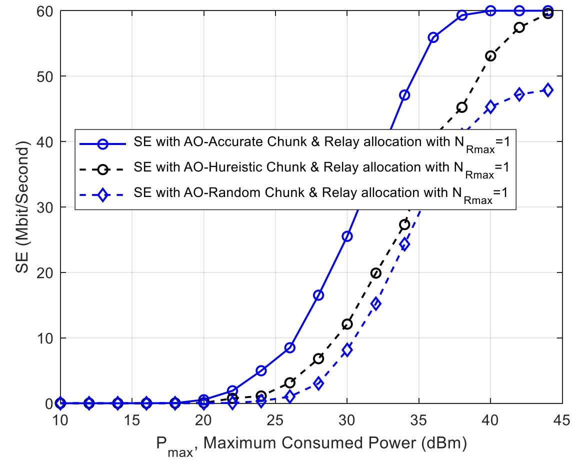

FIGURE 6. (Average) SE results versus P_{max}: using accurate vs. heuristic chunk allocation and relay selection with δ_m as in case 2.

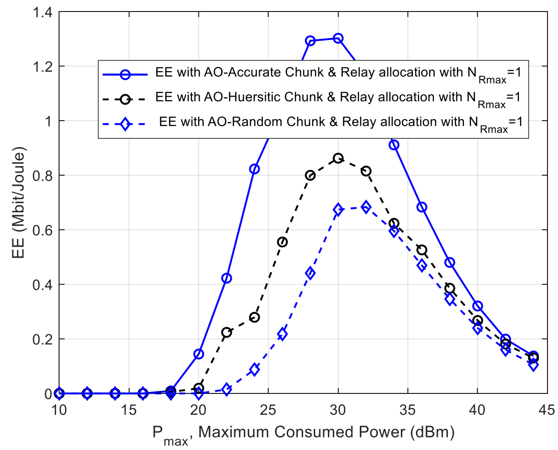

FIGURE 7. (Average) EE results versus P_{max}: using accurate vs. heuristic chunk allocation and relay selection with δ_m as in case 2.

and SE. Both EE and SE show identical increasing behavior for the limited power budget of $P_{max} < 30$ dBm, and for $P_{max} = 30$ dBm, EE has its maximum value. However, increasing the level of P_{max} further and for the rich transmit power of $P_{max} \geq 30$ dBm, the EE level drops significantly, whereas SE has a rising trend (increases) until it reaches its saturation value at $P_{max} = 40$ dBm. For $P_{max} \geq 40$ dBm, both SE and EE level off at a peak value and local peak respectively. The minimum requirement of the SE (the $\overline{S_1}$ parameter in (28)) is assumed to be 40 active subcarriers per chunk.

The reason behind the observed EE trend is rooted in our three-stage optimization approach detailed in Section V. For a given P_{max}, we first optimize SE and then maximize EE using the DKB algorithm with the optimized SE as a fixed input. Consequently, in this SE-oriented EE optimization approach —also discussed in [59] and [24]—, once P_{max} becomes sufficiently large to reach the global EE maximum (e.g., $P_{max} \geq 30$ dBm), any additional transmit power is no longer utilized for the sake of the maximum EE.

Experimental results in Fig. 3, and Fig. 4 suggest that through the appropriate selection of P_{max}, we can achieve an optimal operation point in terms of the network SE, and the network EE. The operational point of $P_{max} = 33.6$ dBm, located between the peak point of the EE curve (Fig. 4) and the knee point of the SE curve (Fig. 3), can be a preferable design point. For this, EE is around its maximum value (0.9 Mb/J), and SE is around 48 Mb/s, which is around 66% (two-thirds) of its peak value.

Overall, across all P_{max} regimes, Figs. 3 and 4 reveal that increasing the δ_m value results in a decreasing trend for both SE and EE.

Overall, a general trade-off is often observed between SE and EE; however, our proposed three-stage optimization framework is designed to mitigate this trade-off effectively.

As explained in Section V, the maximization of EE in Equation (26) is carried out in two core optimization phases. First, SE (the numerator of Equation (26)) is optimized through joint chunk allocation and relay selection using AO algorithm. Notably, SE in this context is independent of the relay power variable $P_{R,r}[k]$, whereas the total power consumption P_T (the denominator) depends on $P_{R,r}[k]$. In the second phase, we apply the DKB algorithm to determine the optimal value of $P_{R,r}[k]$ that maximizes EE with a given P_{max}, using the previously optimized SE as a fixed input. EE is then computed as the ratio of the fixed SE to the optimized P_T. This sequential process ensures that throughput remains high while minimizing power consumption, as detailed in Section V and supported by the results shown in Figures 5–7.

The observed trends in SE (Fig. 6) and EE (Figs. 5 and 7) are consistent with those reported in [59], despite several differences in evaluation methodology and system configuration, namely, our use of GEE versus WSEE in [59], and chunk-level versus subcarrier-level resource processing.

Our method aligns with the spectral-efficiency-maximization (SEM)-based EE optimization approach described in [59] and [24]. In both cases, EE reaches a peak at a certain relay power level P_{max}, beyond which further increases in power no longer improve EE. This explains why, in our results, increasing transmit power beyond P_{max} (e.g., ≥30 dBm) does not lead to higher EE, as the additional power is not used for the sake of the maximum EE. Indeed, as seen in our results, as the total power P_{max} is increased, our SEM-oriented algorithm continues to consume all the available transmit power to achieve a higher system capacity and the algorithm does not continue to allocate the redundant power for the sake of the maximum energy efficiency. This algorithm enables improved EE without sacrificing throughput, already optimized in Stage 2 of Section V.

C. COMPARING THE SUBOPTIMAL AND DKB POWER CONTROL METHODS

In another experiment, we evaluated the performance of using two power control (PC) methods: 1) the suboptimal method and 2) the DKB algorithm. Since SE is not a function of $P_{R,r}[k]$, only EE is affected by $P_{R,r}[k]$ calculations. We benchmark the suboptimal scheme against DKB-based algorithm, as shown in Fig. 5. It is seen that the DKB algorithm yielded higher EE because it integrates constraint C'_3 in (26) during solving the optimization problem, while the suboptimal method, first solves the unconstraint problem and then enforces the results to guarantee the constraint C'_3 in (26), by performing another stage of subcarrier suppression, further scarifying the SE. To be precise, the suboptimal method's EE is close to the DKB algorithm, except for $P_{max} < 30$ dBm. This is because for higher value of $P_{max} \geq 30$ dBm, the constraint C'_3 in (26) is respected, achieving the same results for both PC algorithms, while for the cases of $P_{max} < 30$ dBm, there are violations in the constraint C'_3 in (26). Meanwhile, in our operating point of $P_{max} = 33.6$ dBm, the suboptimal method's EE is very close to the DKB algorithm. Hence, because of simplicity and less complexity, except for the case of Fig. 5, the suboptimal method for power control is used in all of our evaluations.

D. COMPARING ACCURATE AND HEURISTIC CHUNK ALLOCATION AND RELAY SELECTION METHODS

In another experiment, we compared three chunk-level allocation methods—accurate, heuristic, and random—within the AO loop using subcarrier-level power control to assess their impact on SE and EE. As shown in Figs. 6 and 7, the accurate method (via MATLAB's MILP solver) consistently outperforms both heuristic and random-based approaches.

To further examine the accurate and heuristic chunk allocation and relay selection methods, Table 2 compares results from the accurate optimization solver with our proposed heuristic approaches using the AO method. The allocated chunks C_m and selected relays R_m for paired UEs (A_m, B_m), $m = 1, 2, \ldots, M$, differ between the two approaches. The reason for this issue is that the proposed heuristic algorithms of chunk allocation and relay selection are in the class of greedy algorithms, which try to find local optimal solutions in the hope of finding global optimal solutions. However, for many optimization problems, greedy algorithms fail to find the globally optimal solution [60]. As a result, for some P_{max} values, the heuristic algorithms do not guarantee convergence to an optimal solution within n_{AO} iterations of the AO algorithm. This leads to suboptimal chunk allocation and relay selection, ultimately failing to guarantee the stability and optimality of the energy efficiency (EE) solution.

TABLE 2. Simulation results for the joint chunk allocation and relay selection for the case of P_{max}= 33.6 dBm.

Chunk allocation & relay selection method	Allocated chunks, C_m for different paired UEs, m=1,2,…., M	Selected relays, R_m for different paired UEs, m=1,2,…., M
AO-accurate algorithm	[1 6 7 3 2 4 5 8]	[8 4 3 6 2 5 1 7]
AO-heuristic algorithm	[7 6 8 1 4 3 2 5]	[1 8 6 5 7 3 2 4]

E. COMPUTATIONAL COMPLEXITY OF THE PROPOSED FRAMEWORK

In the OFDMA-PNC system of this work the total available bandwidth is divided into N orthogonal subcarriers (e.g., N = 512), which are grouped into $C = N/N_1$ chunks, where each chunk consists of N_1 consecutive subcarriers (e.g., $N_1 = 64$, $C = N/N_1 = 8$). In the considered setup, each of the M user equipment (UE) pairs (e.g., $M = C = 8$) is allocated a dedicated chunk and served via one of the R available relay nodes. Thus, the number of active UE pairs is equal to the number of available chunks, with each chunk supporting a bidirectional transmission session under the DF-PNC protocol.

In the exact formulation, both the chunk allocation and relay selection subproblems are modeled as mixed-integer linear programming (MILP) problems and solved using CVX, which typically relies on the branch-and-bound method. Let C denote the number of chunks and *R* the number of available relays. Then, the worst-case complexity per AO iteration is $O(2^C + 2^R)$ [61], [62], reflecting the exponential growth of the binary decision space for MILPs. Following the AO stage, the DKB algorithm is applied to solve a nonlinear fractional programming (NLP) problem, where the objective is the ratio of total system throughput to overall power consumption. At each iteration of the DKB algorithm, a subtractive-form convex NLP is solved using CVX. Let n_{DKB} denote the number of DKB iterations and let c and m represent the number of continuous power allocation variables (c = N) and constraints (m = 4), respectively. The complexity of this stage is $O(n_{DKB}Q(c, m))$, where $Q(c, m) = (c + m)^3$ denotes the per-stage polynomial complexity of solving a convex NLP using interior-point methods, as implemented in MATLAB's fmincon solver, and supported by the theoretical analysis of interior-point algorithms presented in [63], [64].

To ensure scalability, we also design low-complexity heuristic algorithms for both stages. In the AO stage, a binary decision tensor $X \in \{0, 1\}^{C \times R \times M}$ representing chunk–relay–user assignments are reordered based on link quality metrics (e.g., the number of good subcarriers on each chunk), enabling a greedy yet feasible allocation process. The resulting heuristic has a computational complexity of $O(CM\log_2 M + RM\log_2 M)$, primarily due to sorting and assignment steps. In the power control stage, a heuristic reordering of subcarriers based on per-subcarrier energy efficiency is used, followed by a simplified greedy power allocation algorithm. This results in a complexity of $O(MN_1\log_2 N_1 + NM)$.

In summary, the total computational complexity of the proposed framework depends on the solution strategy. When exact CVX-based solvers are used, the overall worst-case complexity is $O(n_{AO}(2^C + 2^R) + n_{DKB}(N+4)^3)$, where n_{AO} is the number of AO iterations. In contrast, the heuristic-based implementation significantly reduces the complexity to $O(n_{AO}(CM\log_2 M + RM\log_2 M) + MN_1\log_2 N_1)$.

This hybrid design provides a flexible trade-off between solution accuracy and computational efficiency, making the framework well-suited for benchmark-grade evaluation and large-scale deployment in OFDMA-based DF-PNC relay networks.

Despite the high computational cost, the exact method offers notable performance benefits in our OFDMA-PNC scenario, where user equipment operates at a maximum transmit power of 33.6 dBm. Specifically, it achieves an 85% improvement in spectral efficiency and a 47% gain in energy efficiency over the heuristic approach. However, this significant performance gain comes at the expense of much higher complexity, making the exact method less suitable for real-time or large-scale deployments.

VII. CONCLUSION

This paper has presented a novel and comprehensive optimization framework for radio resource allocation in multi-user, multi-relay OFDMA-PNC systems, targeting both spectral efficiency and energy efficiency objectives. A joint approach, integrating chunk-level SE-based chunk allocation, relay selection, and subcarrier-level EE power control, was proposed to address the underlying computationally intensive, NP-hard MINLP problem inherent to these systems. By decoupling the optimization variables and leveraging both accurate (MILP-based) and heuristic algorithms through an AO strategy, the proposed solution achieves a practical balance between performance and computational complexity.

Extensive numerical experiments validated the effectiveness of the proposed joint allocation framework. At a typical operating point of $P_{max} = 33.6$ dBm, the exact AO-based method achieves substantial performance gains over heuristic approaches, including up to 85% higher spectral efficiency and 47% higher energy efficiency. The results also highlight and quantify the SE–EE trade-off, showing that the proposed two-stage optimization process can effectively mitigate this trade-off and achieve close-to-optimal efficiency in both metrics. Comparative analysis of chunk allocation and relay selection techniques further confirmed that the accurate MILP-based solution consistently outperforms heuristic and random assignment, albeit at increased computational cost. Detailed complexity analyses were presented for both accurate and heuristic variants, providing guidance on their selection for different deployment scenarios.

In summary, this work provides a scalable, efficient, and flexible resource allocation strategy for modern OFDMA-PNC systems, supporting the design and deployment of energy- and spectrum-efficient relay-assisted wireless networks in 5G and beyond. The framework is broadly applicable to systems where stringent energy consumption and throughput constraints coexist.

APPENDIX
CALCULATING δ^M PARAMETER

Assuming a chunk-level constant value for δ_m, as a chunk-level power scaling parameter, this parameter is a function of $P'_{max} = P_{max}/\eta_m$ and the channel gains on the subcarriers of each chunk. We propose a definition for δ_m based on the channel gain parameter, as inspired by the approaches outlined in [45], as follows.

By allocating more power to the weaker subcarriers, and without loss of generality, assuming $|H_{A_mR}[k]| \le |H_{B_mR}[k]|$, we set $P'_{A_m}[k] = P''_{max} \ge P_{B_m}[k]$, where P''_{max} represents the maximum average power per subcarrier available at the transmitter side. Further, assuming equal maximum power across different subcarriers (i.e., $P''_{max} = \frac{P'_{max}}{N_1}$), we define the chunk-level power scaling parameter, δ_m as follows:

$$\delta_m = \frac{\sum_{k=1}^{N_1} \delta_m[k]}{N_1}, \tag{43}$$

where

$$\delta_m[k] = \frac{\eta_m P_{max}}{N_1 P_{s1}} \mathrm{Min}\{|H_{A_mR}[k]|^2, |H_{B_mR}[k]|^2\}, \forall k \in \{1, 2, \ldots, N_1\}, \tag{44}$$

is the subcarrier-level power scaling factor.

UPPER BOUND AND LOWER BOUND OF δ_M

Using the subcarrier suppression method, only N_{1used}, and N_{2used} out of N_1 subcarriers of each chunk are utilized for each m-th UE pair (A_m, B_m). Thus, the total power for the m-th UE pair can be expressed as follows:

For user A_m:

$$\sum_{k=1}^{N_1} P'_{A_m}[k] = \sum_{k=1}^{N_{1used}} \frac{\delta_m P_{s1}}{\eta_m |H_{A_mR}[k]|^2} \le P'_{max}. \tag{45}$$

From this inequality, we derive,

$$\delta_m \leq \frac{\eta_m P'_{max}}{P_{s1}.\sum_{k=1}^{N_{1used}} \frac{1}{|H_{A_mR}[k]|^2}}. \tag{46}$$

For user B_m,

$$\sum_{k=1}^{N_1} P'_{B_m}[k] = \sum_{k=1}^{N_{2used}} \frac{\delta_m P_{s1}}{\eta_m |H_{B_mR}[k]|^2} \leq P'_{max}. \tag{47}$$

Similarly, this leads to

$$\delta_m \leq \frac{\eta_m P'_{max}}{P_{s1} \sum_{k=1}^{N_{2used}} \frac{1}{|H_{B_mR}[k]|^2}}. \tag{48}$$

The inequalities (46), and (48) can be simplified as

$$\delta_m \leq \delta_{m,Max1} = \frac{\eta_m P'_{max}}{P_{s1}}.Min\left\{\frac{1}{\sum_{k=1}^{N_{1used}} \frac{1}{|H_{A_mR}[k]|^2}} \frac{1}{\sum_{k=1}^{N_{2used}} \frac{1}{|H_{B_mR}[k]|^2}}\right\}. \tag{49}$$

Here, we use consumed power instead of transmit power of the UEs in our formulization; hence, the m-th UE pair transmit power levels $P_{A_m}[k] = \frac{\delta_m P_{s1}}{|H_{A_mR}[k]|^2}$ and $P_{B_m}[k] = \frac{\delta_m P_{s1}}{|H_{B_mR}[k]|^2}$ is transformed into $P'_{A_m}[k] = \frac{P_{A_m}[k]}{\eta_m}$ and $P'_{B_m}[k] = \frac{P_{B_m}[k]}{\eta_m}$, where η_m is the m-th UE pair power amplifier (PA) efficiency.

On the other hand, to ensure successful decoding of the received signals at the relay and to perform accurate PNC mapping, the relay side SNR must meet the following requirement. Using equation (9), the SNR at the relay R_r is given by:

$$SNR_{R,r} = \frac{MP'_s \delta_m}{\sigma_t^2} \geq SNR_{Min}. \tag{50}$$

To satisfy this condition, the power allocation factor δ_m must be:

$$\delta_m \geq \delta_{Min} = \frac{\sigma_t^2}{MP'_s} SNR_{Min} \tag{51}$$

where SNR_{Min} is the predetermined minimum SNR required at the relay for the correct decoding of the messages.

Combining (7), (49), and (51), we have the following bounds for δ_m,

$$\delta_{Min} \leq \delta_m \leq \delta'_{mMax} = Min\{1, \delta_{m,Max1}\}. \tag{52}$$

To achieve energy-efficient power control, an optimal middle value of δ_m (as in (52)) should be selected using an optimization method. This issue is explored in Section VI-B.

REFERENCES

[1] F. Tan, T. Lv, and S. Yang, "Power allocation optimization for energy-efficient massive MIMO aided multi-pair decode-and-forward relay systems," *IEEE Trans. Commun.*, vol. 65, no. 6, pp. 2368–2381, Jun. 2017.

[2] S. Zhang, S. C. Liew, and P. P. Lam, "Hot topic: Physical layer network coding," in *Proc. Int. Conf. Mobile Comput. Netw.*, Los Angeles, CA, USA, Sep. 2006, pp. 358–365.

[3] P. Popovski and H. Yomo, "The anti-packets can increase the achievable throughput of a wireless multi-hop network," in *Proc. IEEE Int. Conf. Commun. (ICC)*, 2006, pp. 3885–3890.

[4] H. Thomsen, E. De Carvalho, and P. Popovski, "Emulating wired backhaul with wireless network coding," in *Proc. URSI General Assembly Sci. Symp. (URSI GASS)*, Beijing, China, 2014, pp. 1–4.

[5] H. Zhang, Y. Liu, and M. Tao, "Resource allocation with subcarrier pairing in OFDMA two-way relay networks," *IEEE Wireless Commun. Lett.*, vol. 1, no. 2, pp. 61–64, Apr. 2012.

[6] R. Y. Chang, S.-J. Lin, and W.-H. Chung, "Symbol and bit mapping optimization for physical-layer network coding with pulse amplitude modulation," *IEEE Trans. Wireless Commun.*, vol. 12, no. 8, pp. 3956–3967, Aug. 2013.

[7] E. A. Doost, F. B. Saghezchi, S. Mumtaz, J. Rodriguez, and L. Musavian "OFDM-based synchronous PNC communications using higher order QAM modulations," in *Proc. IEEE Int. Conf. Commun. (ICC)*, Rome, Italy, 2023, pp. 1444–1449.

[8] S. Pizzi, F. Rinaldi, A. Molinaro, A. Iera, and G. Araniti, "Energy-efficient multicast service delivery exploiting single frequency device-to-device communications in 5G new radio systems," *Sensors*, vol. 18, no. 7, p. 2205, 2018.

[9] A. R. Castro e Souza, J. R. de Almeida Amazonas, and T. Abrao, "Energy-efficiency maximisation for cooperative and non-cooperative OFDMA cellular networks—A survey," *Wiley Trans. Emerg. Telecommun. Technol.*, vol. 27, no. 2, pp. 216–248, 2016.

[10] S. Buzzi, I. Chih-Lin, T. E. Klein, H. V. Poor, C. Yang, and A. Zappone, "A survey of energy-efficient techniques for 5G networks and challenges ahead," *IEEE J. Sel. Areas Commun.*, vol. 34, no. 4, pp. 697–709, Apr. 2016.

[11] S. Kim and H. Yu, "Energy-efficient resource allocation in multi-user AF two-way relay channels," *J. Commun. Netw.*, vol. 18, no. 4, pp. 629–638, Aug. 2016.

[12] M. Ding, S. Atapattu, C. Weeraddana, and J. Evans, "Energy-efficiency fairness of interference multi-relay networks for multi-user communications," *IEEE Commun. Lett.*, vol. 25, no. 3, pp. 955–959, Mar. 2021.

[13] L. Sboui, Z. Rezki, A. Sultan, and M. -S. Alouini, "A new relation between energy efficiency and spectral efficiency in wireless communications systems," *IEEE Wireless Commun.*, vol. 26, no. 3, pp. 168–174, Jun. 2019.

[14] B. Bossy, P. Kryszkiewicz, and H. Bogucka, "Energy-efficient OFDM radio resource allocation optimization with computational awareness: A survey," *IEEE Access*, vol. 10, pp. 94100–94132, 2022.

[15] Y. Liu, J. Mo, and M. Tao, "QoS-aware transmission policies for OFDM bidirectional decode-and-forward relaying," *IEEE Trans. Wireless Commun.*, vol. 12, no. 5, pp. 2206–2216, May 2013.

[16] S. Dang, M. Wen, S. Mumtaz, J. Li, and C. Li, "Enabling multicarrier relay selection by sensing fusion and cascaded ANN for intelligent vehicular communications," *IEEE Sensors J.*, vol. 21, no. 14, pp. 15614–15625, Jul. 2021.

[17] A. Kurdija, M. Smiljanic, and Z. Ilic, "A chunk and power allocation algorithm for proportional fairness in OFDMA relay networks," *Wireless Netw.*, vol. 22, pp. 2741–2751, Nov. 2015.

[18] M. Saito, S. Haraguchi, and M. Okada, "Dual-hop non-regenerative OFDM relay systems with chunk-based power allocation," *Wireless Pers. Commun.*, vol. 64, no. 1, pp. 51–64, May 2012.

[19] M. Herdin, "A chunk based OFDM amplify-and-forward relaying scheme for 4G mobile radio systems," in *Proc. IEEE Int. Conf. Commun. (ICC)*, Istanbul, Turkey, 2006, pp. 4507–4512.

[20] K. Singh, A. Gupta, and T. Ratnarajah, "A utility-based joint subcarrier and power allocation for green communications in multi-user two-way regenerative relay networks," *IEEE Trans. Commun.*, vol. 65, no. 9, pp. 3705–3722, Sep. 2017.

[21] Y. Shen, Y. Shi, J. Zhang, and K. B. Letaief, "LORM: Learning to optimize for resource management in wireless networks with few training samples," *IEEE Trans. Wireless Commun.*, vol. 19, no. 1, pp. 665–679, Jan. 2020.

[22] V. Tentu, D. N. Amudala, A. Rajoriya, E. Sharma, and R. Budhiraja, "Energy efficient multi-pair massive MIMO two-way AF relaying: A deep learning approach," in *Proc. Int. Conf. Commun. Syst. Netw. (COMSNETS)*, Bengaluru, India, 2020, pp. 440–445.

[23] J. Qu, Y. Cai, and W. Yang, "Energy-efficient joint resource allocation in two-way OFDM relay systems," in *Proc. IEEE 3rd Int. Conf. Inf. Sci. Technol. (ICIST)*, Yangzhou, China, 2013, pp. 1237–1241.

[24] Z. K. Zhou and Q. Zhu, "Joint energy-efficient power allocation and subcarrier pairing in orthogonal frequency division multiple-based multi-relay networks," *IET Commun.*, vol. 9, no. 5, pp. 649–657, Apr. 2015.

[25] K. Singh, A. Gupta, S. Biswas and T. Ratnarajah, "A unified approach towards green resource allocation in relay-assisted multiuser networks," in *Proc. IEEE Global Commun. Conf. (GLOBECOM)*, 2017, pp. 1–6.

[26] K. Singh, M.-L. Ku, and C.-M. Yu, "Joint subcarrier pairing and power allocation for achieving energy-efficient decode-and-forward relay networks," in *Proc. IEEE 89th Veh. Technol. Conf. (VTC-Spring)*, Kuala Lumpur, Malaysia, 2019, pp. 1–6.

[27] A. Zappone, S. Atapattu, M. Di Renzo, J. Evans, and M. Debbah, "Energy-efficient relay assignment and power control in multi-user and multi-relay networks," *IEEE Wireless Commun. Lett.*, vol. 7, no. 6, pp. 1070–1073, Dec. 2018.

[28] S. Zhang, X. Xu, M. Sun, X. Tang, and X. Tao, "Energy efficient uplink transmission for UE-to network relay in heterogeneous networks," in *Proc. IEEE 28th Annu. Int. Symp. Personal, Indoor, Mobile Radio Commun. (PIMRC)*, Montreal, QC, Canada, 2017, pp. 1–7.

[29] K. Singh, A. Gupta, and T. Ratnarajah, "QoS-driven energy-efficient resource allocation in multiuser amplify-and-forward relay networks," *IEEE Trans. Signal Inf. Process. Netw.*, vol. 3, no. 4, pp. 771–786, Dec. 2017.

[30] K. Singh, A. Gupta, T. Ratnarajah, and M.-L. Ku, "A general approach toward green resource allocation in relay-assisted multiuser communication networks," *IEEE Trans. Wireless Commun.*, vol. 17, no. 2, pp. 848–862, Feb. 2018.

[31] I. Basturk, Y. Chen, and M. Alouini, "Energy-efficient communication for user-relay aided cellular networks with OFDMA," *Phys. Commun.*, vol. 33, pp. 153–164, Apr. 2019.

[32] S. Atapattu, Y. Jing, H. Jiang, and C. Tellambura, "Relay selection schemes and performance analysis approximations for two-way networks," *IEEE Trans. Commun.*, vol. 61, no. 3, pp. 987–998, Mar. 2013.

[33] I. Krikidis, "Relay selection for two-way relay channels with MABC DF: A diversity perspective," *IEEE Trans. Veh. Tech.*, vol. 59, no. 9, pp. 4620–4628, Nov. 2010.

[34] K. Singh, A. Gupta, M.-L. Ku, and T. Ratnarajah, "Joint subcarrier pairing and power allocation for two-way energy-efficient relay networks," in *Proc. IEEE Global Commun. Conf. (GLOBECOM)*, Washington, DC, USA, Dec. 2016, pp. 1–6.

[35] K. Singh, A. Gupta, and T. Ratnarajah, "Green resource allocation and EE-balancing in multiuser two-way amplify-and-forward relay networks," in *Proc. IEEE Int. Conf. Commun. (ICC)*, Paris, France, 2017, pp. 1–6.

[36] K. Singh, A. Gupta, and T. Ratnarajah, "QoS-driven resource allocation and EE-balancing for multiuser two-way amplify-and-forward relay networks," *IEEE Trans. Wireless Commun.*, vol. 16, no. 5, pp. 3189–3204, May 2017.

[37] A. Thampi, S. C. Liew, S. Armour, Z. Fan, L. You, and D. Kaleshi, "Physical-layer network coding in two-way heterogeneous cellular networks with power imbalance," *IEEE Trans. Veh. Technol.*, vol. 65, no. 11, pp. 9072–9084, Nov. 2016.

[38] G. Bartoli, R. Fantacci, D. Marabissi and R. Simoni, "Physical layer network coding in multipath channel: Effective precoding-based transmission scheme," in *Proc. IEEE Global Commun. Conf. (GLOBECOM)*, Houston, TX, USA, 2011, pp. 1–5.

[39] S. M. M. Yang, *Modern Digital Radio Communication Signals and Systems*, 2nd ed. Cham, Switzerland: Springer, 2021.

[40] S. Cao and F. Hou, "On the maximum energy efficiency of random access-based OMA and NOMA in multirate environment," *IEEE Trans. Wireless Commun.*, vol. 21, no. 12, pp. 10438–10454, Dec. 2022.

[41] E. Atefat Doost, F. B. Saghezchi, A. Navarro, and J. Rodriguez, "Bit error rate for physical-layer network coding with M-QAM-OFDM signals," *IEEE Wireless Commun. Lett.*, vol. 14, no. 1, pp. 153–157, Jan. 2025.

[42] W. Shin, N. Lee, J. B. Lim, and C. Shin, "An optimal transmit power allocation for the two-way relay channel using physical-layer network coding," in *Proc. IEEE Int. Conf. Commun. Workshops*, Dresden, Germany, 2009, pp. 1–6.

[43] L. K. S. Jayasinghe, N. Rajatheva, and M. Latva-aho, "Optimal power allocation for PNC relay based communications in cognitive radio," in *Proc. IEEE Int. Conf. Commun. (ICC)*, Kyoto, Japan, 2011, pp. 1–5.

[44] Z. Chang, Q. Zhang, X. Guo, and T. Ristaniemi, "Energy-efficient resource allocation for OFDMA two-way relay networks with imperfect CSI," *EURASIP J. Wireless Commun. Netw.*, vol. 2015, p. 225, Oct. 2015.

[45] G. Bartoli, R. Fantacci, D. Marabissi, and R. Simoni, "Subcarriers suppression methods for OFDM systems with decode-and-forward network coding," *IEEE Trans. Wireless Commun.*, vol. 12, no. 12, pp. 6034–6042, Dec. 2013.

[46] X. Shen, K. Xu, W. Ma, and Y. Xu, "Joint subcarriers suppression and relay selection in PLNC based two-way OFDM relaying system," in *Proc. 6th Int. Conf. Wireless Commun. Signal Process. (WCSP)*, Hefei, China, 2014, pp. 1–6.

[47] M. Grant and S. Boyd, "CVX: MATLAB software for disciplined convex programming, version 2.2." Jan. 2020. [Online]. Available: http://cvxr.com/cvx

[48] "CPLEX," 2024. [Online]. Available: http://www.ilog.com/products/cplex

[49] *MATLAB Optimization ToolboxTM User's Guide (R2023a)*. The MathWorks, Inc., Natick, MA, USA, Jul. 2023.

[50] Y. Shen, Y. Shi, J. Zhang, and K. B. Letaief, "Graph neural networks for scalable radio resource management: Architecture design and theoretical analysis," *IEEE J. Sel. Areas Commun.*, vol. 39, no. 1, pp. 101–115, Jan. 2021.

[51] J. Zhang et al., "A survey for solving mixed integer programming via machine learning," *Neurocomputing*, vol. 519, pp. 205–217, Jan. 2023.

[52] A. Zappone and E. A. Jorswieck, "Energy-efficient resource allocation in future wireless networks by sequential fractional programming," *Digit. Signal Process.*, vol. 60, pp. 324–337, Jan. 2017.

[53] W. Dinkelbach, "On nonlinear fractional programming.," *Manage. Sci.*, vol. 13, no. 7, pp. 492–498, Mar. 1967.

[54] A. Charnes and W. W. Cooper, "Programming with linear fractional functionals," *Naval Res. Logist. Quart.*, vol. 9, nos. 3–4, pp. 181–186, Sep./Oct. 1962.

[55] F. Tan, H. Chen, F. Zhao, and X. Li, "Energy-efficient power allocation for massive MIMO-enabled multi-way AF relay networks with channel aging," *EURASIP J. Wireless Commun. Netw.*, vol. 2018, no. 1, pp. 206–226, Dec. 2018.

[56] A. Zappone and E. Jorswieck, "Energy efficiency in wireless networks via fractional programming theory," *Found. Trends Commun. Inf. Theory*, vol. 11, no. 3, pp. 185–396, 2015.

[57] J. Zhang, M. Ding, D. López-Pérez, A. Marshall, and L. Hanzo, "Design of an efficient OFDMA-based multi-user key generation protocol," *IEEE Trans. Veh. Tech.*, vol. 68, no. 9, pp. 8842–8852, Sep. 2019.

[58] "Study on channel model for frequencies from 0.5 to 100 GHz," 3GPP, Sophia Antipolis, France, Rep. TR 38.901, V17.0.0, 2022.

[59] S. Kim and Y. H. Lee, "Energy-efficient power allocation for OFDM signaling over a two-way AF relay," *IEEE Trans. Veh. Technol.*, vol. 64, no. 10, pp. 4856–4863, Oct. 2015.

[60] T. H. Cormen, C. E. Leiserson, R. L. Rivest, and C. Stein, *Introduction to Algorithms*, 4th ed. Cambridge, MA, USA: MIT Press, 2022.

[61] J. V. Saraiva, F. R. Lima, A. M. Pessoa, T. F. Maciel, W. D. Junior, and F. R. Cavalcanti, "Energy-efficient radio resource allocation for dual-hop relay-assisted orthogonal frequency division multiple access systems with quality of service provisioning," *Trans. Emerg. Telecommun. Technol.*, vol. 32, no. 10, pp. 1–31, 2021.

[62] N. Thakoor and J. Gao, "Branch-and-bound for model selection and its computational complexity," *IEEE Trans. Knowl. Data Eng.*, vol. 23, no. 5, pp. 655–668, May 2011.

[63] F. A. Potra and S. J. Wright, "Interior-point methods," *J. Comput. Appl. Math.*, vol. 124, no. 1-2, pp. 281–302, Dec. 2000.

[64] S. Sharif, M. Liaq, and W. Ejaz, "Multi-objective resource optimization in space-aerial-ground-sea integrated networks," in *Proc. IEEE Symp. Wireless Technol. Appl. (ISWTA)*, 2023, pp. 109–114.

EHSAN ATEFAT DOOST received the B.Sc. and M.Sc. degrees in electrical engineering from Shiraz University, Shiraz, Iran, in 1998 and 2001, respectively. He is currently pursuing the Ph.D. degree with the University of Aveiro, Portugal. His research interests include signal processing and radio resource management in wireless communication systems.

FIROOZ B. SAGHEZCHI (Senior Member, IEEE) received the Ph.D. degree in telecommunications engineering from the University of Aveiro, Portugal, in 2016. From 2010 to 2023, he was a Research Fellow with the Instituto de Telecomunicações, Portugal. Since 2023, he has been with the Chair for Distributed Signal Processing, RWTH Aachen University, Germany, as a Senior Researcher. His research interests include signal processing, machine learning, and resource allocation.

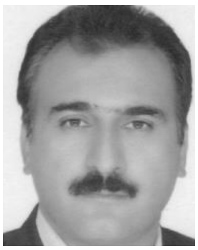

ALI JAMSHIDI (Senior Member, IEEE) received the B.S. degree in electrical engineering from Shiraz University, Shiraz, Iran, in 1997, and the M.S. and Ph.D. degrees in electrical engineering from the Sharif University of Technology, Tehran, Iran, in 1999 and 2007, respectively. He joined Shiraz University in 2007, where he is currently an Associate Professor with the Department of Communications and Electronics, School of Electrical and Computer Engineering. He is also the Director of the Software Defined Radio Center, School of Electrical Engineering, Shiraz University. His current research interests include wireless communication research areas, such as wireless communication signal processing, underwater acoustic communications, cognitive radio, cooperative communication, relay systems, nano and molecular communications, and communication intelligence systems. He serves as a Reviewer for the IEEE TRANSACTIONS ON VEHICULAR TECHNOLOGY, the *IEEE Sensors*, the IEEE TRANSACTIONS ON SIGNAL PROCESSING, and some Elsevier and Springer journals.

ANTONIO NAVARRO (Senior Member, IEEE) graduated in electrical engineering from Coimbra University, Portugal in 1989. He received the M.Sc. degree from the University of Coimbra, Portugal, in 1993, and the Ph.D. degree from the University of Newcastle upon Tyne, U.K. in 1996. He is currently a Professor with the Electronics, Telecommunications and Informatics Engineering Department, Aveiro University, Portugal, where he lectures courses on coding and transmission of video/TV signals, on radio planning as well as on propagation and radiation of electromagnetic waves. He supervised more than 50 postgrad students. He is a co-author of about 200 scientific publications and five granted patents. His research interests are on digital television, RF measurements, video coding, and reliable wireless transmission of video-based multimedia services. He has been awarded ten times for his scientific achievements. He has participated (led half of them) in more than 50 national and international research projects. He has been invited to give tutorials on digital television to spectrum regulators, broadcasters and network operators in Portugal and other countries. He was an Associate Editor of IEEE TRANSACTIONS ON CIRCUITS AND SYSTEMS FOR VIDEO TECHNOLOGY from 2006 to 2011. He was the General Chair of IEEE International Conference on Consumer Electronics in 2008 and 2025, and has served as a reviewer of several IEEE journals.

JONATHAN RODRIGUEZ (Senior Member, IEEE) received the M.Sc. degree in electronic and electrical engineering and the Ph.D. degree from the University of Surrey, U.K., in 1998 and 2004, respectively. Since 2005, he has been a Senior Researcher with the Instituto de Telecomunicações, Aveiro, Portugal. Since 2017, he has been a Professor of Mobile Communications with the University of South Wales, U.K. He is the author of more than 600 scientific publications. His research interests include 5G/6G architectures, spectrum management, and radio resource management.